Article

Minimisation of Environmental Impact of Commercial Aviation in Europe: Hydrogen-Powered Aircrafts

Pavel Sizov[1], Denton Philtjens[2], Jamie Yuen[3], Kunjam[4], Joe Bryant[5]

[1] Student (BSc Economics, 2021-24), Dept. of Economics, UCL, UK; pavel.sizov.21@ucl.ac.uk
[2] Student (BSc Economics, 2021-24), Dept. of Economics, UCL, UK; denton.philtjens.21@ucl.ac.u
[3] Student (BSc Economics, 2021-24), Dept. of Economics, UCL, UK; jamie.yuen.21@ucl.ac.uk
[4] Student (BSc Economics, 2021-24), Dept. of Economics, UCL, UK; kunjam.21@ucl.ac.uk
[5] Student (BSc Economics, 2021-24), Dept. of Economics, UCL, UK; joe.bryant.21@ucl.ac.uk

How to cite
Sizov, P., *et al.* (2024). Minimisation of Environmental Impact of Commercial Aviation in Europe: Hydrogen-Powered Aircrafts. *UCL Journal of Economics*, vol. 3 no. 1. DOI: 10.14324/111.444.2755-0877.1856

Peer review
This article has been peer-reviewed through the journal's standard double-blind peer review, where both the reviewers and authors are anonymised during review

Open access
UCL Journal of Economics is a peer-reviewed open-access journal

Abstract

This paper examines hydrogen-powered aircraft as a means to reduce commercial aviation's long-run environmental impact in Europe, aligning with the EU's 2050 net-zero emissions goal. Focusing on short-haul intra-European flights, our study proposes a network of on-site electrolysers powering a fleet of hybrid hydrogen aircrafts. We model (1) the monetary cost of emissions in aviation, (2) how pollutive flight routes are, and (3) the private (monetary) costs of equipping airports with hydrogen infrastructure and servicing aircrafts. We develop a novel combinatorial optimisation algorithm to select airports to decarbonise across a range of carbon cost cases. We find that €2.79bn in long-run annual welfare can be unlocked under the base case. Finally, we illustrate how an EU-wide kerosene tax is expected to provide an additional €3.13bn long-run annual welfare with this approach.

Keywords: Environment, Hydrogen, Aviation, Networks, Combinatorial Optimisation, Emissions, EU

1. Introduction

1.1. Motivation to tackle global warming

2023 is set to be the warmest year on record, approximately 1.4°C warmer than the pre-industrial baseline (1850-1900) (World Meteorological Organization, 2023). In the 2015 Paris Agreement, 196 nations collectively agreed to target keeping the increase in global average temperature to well below 2°C above pre-industrial levels (Paris Agreement, 2015, Article 2). However, this target will likely not be met because of inadequate pledges from participating countries (Harper, Lam and Dodd, 2021). This has generated significant socio-political pressure, due to the growing public concern over the impacts of climate change and the realisation that urgent action is needed at all levels of society.

In 2018, the European Union (EU) set forth the vision of reaching net zero by 2050 (European Union, 2021, Article 2) which necessitates that all member states take urgent measures to achieve a domestic reduction in net greenhouse gas (GHG) emissions by a minimum of 55% relative to the levels recorded in 1990, by the year 2030. (European Union, 2021, Article 4).

Beyond the environmental incentive for transitioning to more sustainable energy sources, there are also compelling economic reasons - namely to reduce energy market volatility and instability. For instance, the price of the Brent crude oil index increased from 91.41 in February 2022 (prior to the escalation of the Russia-Ukraine conflict) to 123.07 4 months later, the highest level since June 2008 (Business Insider, 2023). These geopolitical conflicts have led alternative energy sources to become more competitive and stable, reinforcing the incentive to shift towards renewable energy.

1.2. Narrowing the scope

Whilst many sectors contribute to global GHG emissions, the transport sector represents one of the largest contributors, accounting for 25% of the EU's total GHG emissions in 2021 (EEA, 2023). Moreover, whilst GHG emissions in the EU fell by 32% between 1990 to 2020, the transport industry's total GHG emissions have grown at a rate of 7% during this same period (Masterson, 2022). Within transport, aviation emissions have grown the fastest, having doubled during this period and having gone from 1.5% of all European emissions in 1990 to 4.7% in 2019 (pre-pandemic), (Transport & Environment, n.d.). If unchecked, aviation emissions could double again by 2050 (Transport & Environment, n.d.).

The aviation industry is thus one of the most pressing to decarbonise, yet simultaneously considered one of the hardest due to the long lifespan of aeroplanes and the significant costs of decarbonisation solutions (Shell, n.d.). Presently, prototypes have been developed using hydrogen, synfuel, biofuel and batteries to try to achieve the "Fly Net Zero" pledge in accordance with the net zero goals set up in the Paris Agreement (IATA, 2021). Out of these proposed solutions, hydrogen is arguably the cleanest fuel which produces mainly water as a by-product and no carbon by-products (Wu, 2022). Notably, green hydrogen aircrafts (hydrogen produced and refined using renewable energy only) can remove 70% to 80% of the climate impact, whereas synfuels and biofuels can only remove 30% to 60% (Fuel Cells and Hydrogen 2 Joint Undertaking [FCH JU], 2020). Moreover, battery-electric aircrafts can only travel 500-1000 km, which would not cover a majority of European air transport (Fuel Cells and Hydrogen 2 Joint Undertaking [FCH JU], 2020).

The scope of our research is further narrowed to focus on short-haul, intra-European flights which depend upon a network of on-site (at airport) hydrogen electrolysers to power a fleet of hybrid aircrafts. To define our geographical scope, this study is limited to investigating flights both departing and landing within the European Union (EU), the United Kingdom and Norway. This geographical scope is referred as EU+ proceeding forward in this paper.

DOI: 10.14324/111.444.2755-0877.1856

We decide to investigate short-haul flights as flights with duration less than 6 hours firstly because they are more carbon intensive per km than long-haul (Anderson, 2023). Moreover, long-haul hydrogen aircrafts require a greater extent of revolutionary modifications, for example requiring a blended-wing-body. Consequently, there will be higher development costs and they are only estimated to enter into service after 2045 (Fuel Cells and Hydrogen 2 Joint Undertaking [FCH JU], 2020). Contrarily, short-haul H2 flights can contribute to reducing GHG emissions much earlier (in line with the EU's goal for 2050) as they are estimated to enter into service between 2030 and 2035 (Fuel Cells and Hydrogen 2 Joint Undertaking [FCH JU], 2020).

We choose to focus on the EU+ region for 4 main reasons. Firstly, almost all intra-EU+ flights are short-haul and compatible with the technological capabilities of H2 aircrafts. Secondly, there was high accessibility to EU+ data for computational and modelling purposes via Eurostat. Thirdly, the region's strong focus on environmental policies means that our suggestions may realistically and tangibly contribute to the groundwork for future policy making. Finally, the region's largest economic and political union, the EU, has a uniform and non-fragmented legislative structure for bill making, which can lead to efficient wide-spread policy implementation.

Additionally, we decided to focus on building a network based on on-site electrolysers as this avoids the significant costs of hydrogen transport, including upfront investment in pipelines, trucking and additional purification plants. Moreover, we avoid the long and challenging process of planning, commissioning, and regulating new hydrogen pipelines (Baldino et al., 2020). Furthermore, the implementation of modular electrolysis plants allows for flexibility regarding future demand and scalability (Hydrogen-powered aviation, 2020). This approach, whilst novel, has already achieved proof of concept. For instance, in September 2023, Groningen Airport Eelde in Northern Netherlands established an on-site modular electrolyser suitable for light aircraft, drones, and ground equipment powered by sustainable green hydrogen (Groningen Airport Eelde, 2023).

Finally, we chose to focus on hybrid hydrogen aircrafts (combining turbines and fuel cells, powered by liquid hydrogen (LH2)) as it optimises the higher power density and efficiency of turbines together with the lower climate impact of fuel cell systems (Fuel Cells and Hydrogen 2 Joint Undertaking [FCH JU], 2020). Specifically, the turbine is sized to deliver major thrust for take-off and climbing whilst the fuel cells are used for cruising and descent. Additionally, we chose liquid H2 (LH2) over compressed gaseous H2 (and non-compressed gas) as it requires half the volume, carries significantly lower tank weight and can lead to potentially faster refuelling times (Fuel Cells and Hydrogen 2 Joint Undertaking [FCH JU], 2020).

1.3. Research Roadmap

We commence our investigation by first establishing the marginal environmental benefits and marginal monetary costs of decarbonising each route and airport. We then apply this to a network model and conduct cost benefit analysis to determine which hubs are optimal to decarbonize. Due to the combination of uncertainty in the timeline to develop operational hydrogen aircraft and the computational complexity of modelling dynamics in combinatorial optimisation, we analyse a static model for the long-term, formulating a strategic plan for airport decarbonisation in 2050. Finally, we model and evaluate an EU+-wide per litre kerosene tax using our model and consider alternative future policies for the region to decarbonise aviation efficiently.

2. Methodology

For our report, the methodology is organised into 3 sections. The first discusses the calculation of the marginal benefit per route, which depends on the emissions saved (converted into monetary terms) by utilising hybrid hydrogen aircrafts in 2050. The second section covers monetary costs involving capital expenditure (CAPEX) and operating expenditure (OPEX). The last section combines these marginal benefits and costs by using a network model to suggest which aircraft routes to decarbonise in 2050 - the long-term. Afterwards, we examine how tax policy can make our strategic plan more viable.

2.1. Net Marginal Environmental Benefit

DOI: 10.14324/111.444.2755-0877.1856

Figure X: How to caption a figure

2.1.1. Environmental impacts of kerosene-based aircrafts

As aforementioned, an aircraft emits various gases and particles which contribute to climate change and global warming. Aside from carbon dioxide (CO2), there are various non-CO2 emissions including nitrogen oxides (NOx), water vapour, sulphur dioxide, soot and the formation of linear contrails and contrail-cirrus (Lee D. S., 2018).

Radiative forcing, and its associated radiative effects, denote the changes in energy flux in the atmosphere because of various emissions. Greenhouse gases produce a warming effect and thus carry positive radiative effects. Conversely, emissions with a cooling effect have negative radiative effects.

CO2 emissions originate from the combustion of hydrocarbon fuels (in our case kerosene). These emissions stay in the upper atmosphere for 50 to 100 years and produce a positive radiative forcing effect (Environmental Protection Agency, n.d.).

NOx emissions arise from chemical reactions occurring at high temperatures in the combustion chamber of jet engines and thus depend on the engine's design. NOx emissions lead to the formation of atmospheric ozone (O3), a gas which carries positive radiative effects (Lee D. S., 2018). However, NOx emissions also form short-lived hydroxyl radicals (OH), which contribute to removing ambient methane (CH4) (which is a greenhouse gas) by about 1 – 2% (Lee D. S., 2018) producing a negative radiative effect. Overall, the combination of the two effects yields a net positive radiative effect (Lee, 2021), and these emissions last less than a month in the upper troposphere and lower stratosphere (ICAO, 2022).

Water vapour is also produced during the combustion of kerosene, a greenhouse gas with positive radiative forcing and atmospheric lifetime of a few days (Lee D. S., 2018).

Sulphur dioxide is produced during the oxidation of sulphur in jet fuel, which leads to sulphuric acid (Brown, 1996). Sulphuric acid forms particles that can reflect solar radiation back to space and thus represents a small negative radiative effect (Lee D. S., 2018). These emissions last in the environment for a few weeks.

Furthermore, aircraft jet engines directly emit solid soot particles which encompass all primary, carbon-containing products from incomplete combustion processes in the engine (IPCC, 1999). Since it contributes to absorbing solar radiation (Bond, 2013), it carries a small positive radiative effect. These emissions last in the environment for only a few days to weeks.

Lastly, contrails form behind cruising aircrafts as line-shaped contrails and transform into cirrus-like clouds or cloud clusters in favourable meteorological conditions (Burkhardt & Kärcher, 2011). They cool the atmosphere during the day and heat the surface during night and thus the net effect depends strongly on daily cloud cover variations (Meerkoetter, 1999), with an atmospheric lifetime no greater than several hours. Lee et al. (2021) reported a net warming effect over the sum of the day/night cycle, but these mechanisms remain highly uncertain.

Beyond the direct emissions from kerosene combustion, there exists substantial indirect emissions from its production process - specifically caused by extraction, fractional distillation and transportation, which are all energy intensive and typically powered by fossil fuels.

2.1.2. Environmental impacts of hydrogen-based aircrafts

In contrast to kerosene-based aircrafts, hybrid hydrogen aircrafts do not generate CO2 as the fuel is not carbon-based. However, H2 turbines still rely on combustion processes and emit NOx, although hydrogen's wider flammability limits enable leaner combustion which results in lower flame temperatures and hence lower NOx emissions. With fuel cells, no NOx is released. (Fuel Cells and Hydrogen 2 Joint Undertaking [FCH JU], 2020)

DOI: 10.14324/111.444.2755-0877.1856

For water vapour, H2 turbines and fuel cells emit more compared to kerosene for the same energy content. In H2 turbines, water vapour is released as a by-product of combustion. For fuel cells, H2 breaks apart at the anode and then electrons travel through the circuit to perform work and recombine at the cathode with the protons and oxygen molecules, forming water (vapour). (Alternative Fuels Data Center, n.d.)

No soot or sulphur dioxide is produced by hybrid hydrogen aircrafts. Regarding contrails, H2 turbines produce ice crystal contrails which precipitate faster and are optically thinner (since they aren't combined with soot unlike conventional aircrafts), thus making their climate effects lower than conventional aircrafts. For H2 fuel cells, the climate effect of contrails is considered even lower because the water vapour produced is colder and can precipitate faster.

Lastly, through the process of constructing hydrogen-aircraft related infrastructure (electrolysers, liquefiers, distribution pipeline etc.) at various airports globally, CO2 will be released (as most construction processes run off fossil fuels). Due to data limitations, we cannot feasibly examine this and thus assume that the indirect effects of kerosene production and hydrogen infrastructure approximately equate and cancel out.

2.1.3. Benchmarking Emissions, linking ERF and GWP

Greenhouse gases contribute to global warming via their radiative effects. This is measured and adjusted for short-term variations from feedback effects to derive effective radiative forcing (ERF), which is in turn used to compute values of global warming potential with respect to a 100-year time horizon (GWP100). GWP100 averages the warming potential over a 100-year time frame and is the internationally accepted standard, used by the United Nations in the Kyoto Protocol. GWP100 quantifies the warming effects of any greenhouse gas as a multiple of the warming effect of CO2 (of the same mass), allowing greenhouse gasses' warming to be measured as "CO2 equivalent (CO2e)" effects.

To evaluate the effects of various emissions of kerosene aircrafts upon global warming, we adopt the emission indices (kg of emissions per kg kerosene) and respective GWP100 estimated in Skowron, Lee and De León (2015), as shown in Figure 1. For nitrogen oxides, we utilise a GWP100 value specific for Europe.

With this data, by multiplying GWP100 with emission indices, we obtain the amount of emissions of CO22e per kg kerosene for each emission based on 2018 aircraft efficiency.

Additionally, since contrails aren't measured on a per kg basis, we adopt the GWP100 value (0.6) from Lee et al. (2021) and multiply it by the amount of CO2 emitted (3.2 kg/kg kerosene) to calculate CO2e per kilogram kerosene for contrails effect. The CO2e per kilogram kerosene for all emission types is calculated in section 3.

Since our investigation is into the marginal environmental benefit of hydrogen airplanes in 2050, and given the long-term (often multi-century) nature of GWP measures, we assume that GWP100, is unchanged between present day and 2050. We also assume the emission index is unchanged, but we incorporate a 2% p.a. efficiency improvement, in terms of fuel consumption required per km. This is in-line with the goal for efficiency improvements set during the 2010 International Civil Aviation Organization Assembly.

Next, we determine the various emissions produced by hydrogen aircrafts. The gravimetric energy density of hydrogen is 120 MJ/kg, much higher than for Aviation Jet A-1 kerosene (43 MJ/kg). Assuming equally efficient engines, for aircrafts of equivalent size to travel the same distance with the same load, only 0.36kg of hydrogen is needed (43/120). (FCH JU, 2020) provides a comparison of emissions produced by turbines and fuel cells with present day kerosene aircrafts (on a per passenger km basis).

We adopt estimates from (FCH JU, 2020) regarding the percentage changes in climate impact (of hydrogen aircrafts compared to conventional kerosene aircrafts) and the figures for sulphur and soot from Choi (2020) to model the potential changes in climate impact (Figure 2). Given the difference in gravimetric energy density, we compare 1kg of kerosene to 0.36kg of hydrogen, thus holding the potential energy output constant for comparison.

DOI: 10.14324/111.444.2755-0877.1856

This enables us to estimate the amount of emissions avoided per kg kerosene that would have otherwise been combusted if hydrogen alternatives were not employed.

2.1.4. External Cost of CO2

To compare environmental benefits (savings) to monetary costs, we utilise the external cost of CO2 released by the US Government dated February 2021. Their assessment was based on 3 widely cited integrated assessment models (IAM) which differ in assumptions such as the functional form of global mean temperature and sea level rises. Ultimately, they all produce a monetary figure to evaluate the present value for the external costs when an extra tonne of carbon dioxide is emitted (which we apply to our CO2e figure).

Figure 3 (Interagency Working Group on Social Cost of Greenhouse Gases, United States Government, 2021) exhibits the 2050 external cost of CO2 estimated by the report in 2020 US dollars, when the discount rate is set at 2.5%, 3% and 5%, which determines the weight placed upon future damages by converting future damages into present-day value. We convert to 2020 euros using the exchange spot rate on 1st January 2020 (1 USD - 0.8914 EUR) (Exchange Rates UK, 2020).

We believe these values are estimated conservatively as during COP28, the US Environmental Protection Agency (EPA) nearly quadrupled the external cost of carbon dioxide up to $308 (Environmental Protection Agency, 2023) and reduced the central case discount rate to 2%. The lowest estimation in the most recent release ($200/tonne) (with a 2.5% discount rate) is considerably higher than the highest estimate shown in the table ($116/tonne) from the 2021 release. However, we used the 2021 values as the most recent numbers are currently facing scrutiny because the EPA has allegedly “contorted long-standing precedents". (IER, 2023)

2.1.5. Modelling Emission Savings - Determining a “representative aircraft”

To determine which airports should be decarbonised, we firstly determine which routes yield the largest CO2e reduction potential (in kg) annually. Ultimately, we aim to build a relationship where annual passengers (affecting flight frequency) and route distance are inputs and kgCO2e saved is the output. We then apply various growth assumptions to our 2023 emissions to project 2050 emissions.

Firstly, we determine a “representative aircraft” which accounts for the difference between aircrafts in model (technical performance), load factor, interior seating configuration, engine etc. which all affect CO2e emissions and environmental savings. We then determine the representative aircraft’s kgCO2e avoided per passenger kilometre (pkm) (the emissions avoided if it were to be replaced by a hybrid hydrogen aircraft) which is calculated by producing a weighted average based on the aircraft’s “popularity”. “Popularity” is a measure of each model’s proportion of total pkm, where pkm represents the transport of one passenger by 1 km. The total pkm is based on all UK registered aircrafts in 2023, from the “2023 Government Greenhouse Gas Conversion Factors for Company Reporting” (2023 GGR). We acknowledge that this data set does not fully encapsulate the European aviation fleet, but we were limited by the data available.

Next, we also consider how an aircraft’s emissions vary during different parts of the journey - namely climb, cruise and descent. Climbing is the most energy intensive, as the aircraft is accelerating against gravity and transforming chemical energy into gravitational potential energy and kinetic energy. Therefore, turbines (which are more pollutive than fuel cells) are required for this energy intensive phase. Descending is the least energy intensive, as gravitational potential energy is re-converted into kinetic energy.

In general, when an aircraft is cruising, it flies between 31,000 feet to 42,000 feet (Johnston, 2023), typically towards the lower end of that range. For our model, we assume that all aircrafts cruise at 34,000 feet and that it takes the same amount of time per aircraft to climb and descend from that level. According to Givoni and Rietveld (2010), the average climb time for short haul flights is 17.26 minutes and descent time is 17.28 minutes. We acknowledge the limitations of these assumptions, as different aircrafts may be more optimised (in terms of fuel

DOI: 10.14324/111.444.2755-0877.1856

burn) for faster or slower climbs. However, since we are only focusing on short-haul flights where there is less variation in aircraft performance compared to long-haul flights, we believe in the adequacy of adopting an average. The cruising time fully depends on the distance flown.

2.1.5. Modelling Emission Savings - Cruise Phase

We utilise equation (1) below to convert $\frac{fuel\ (kg)}{time\ (min)}$ to $\frac{kgCO_2e\ saved}{pkm}$, which is calculated per aircraft model, and then $\frac{kgCO_2e\ saved}{km \times \#\ seats\ occupied}$ is weighted based on the model's proportion of total pkm. Speed (% Mach) and fuel (kg)/min are sourced from the Eurocontrol Experimental Centre BADA database (which has data on different models for varying flight levels and flight phases). Load factor is sourced from 2020 GGR (because the 2023 version uses COVID level data which does not apply for future projections). Number of seats available ("# seats available") per model on average and the proportion pkm weights are sourced from the 2023 GGR. Further detail on the equation derivation can be found in the appendix 3.

To model total emissions during cruise, we require estimating the distance travelled, which involves subtracting the distance travelled during climb and descent from the route's total distance.

For both climb and descent, we assume all aircrafts travel at a constant angle, at their average calibrated airspeed (from the BADA database, per model). Then, this speed is multiplied (to convert to km/min) by the average climb or descent time from Givoni and Rietveld 2010 to yield distance travelled (the hypotenuse in our case). Assuming all aircrafts cruise at a height of 34,000 feet (10.36km), we apply Pythagorean theorem to calculate the horizontal distance travelled during climb and descent, and then construct a weighted average based on proportion of total pkm. Equation (2) and Figure 4 illustrates this simplified approach to estimating the horizontal distance travelled for the climb phase of the aircraft.

By subtracting the weighted average horizontal distance during climb and descent from the total route distance, we calculate the weighted average horizontal distance travelled during cruise, shown in equation (3).

2.1.5. Modelling Emission Savings - Climb and Descent Phases

For climb and descent, additional complexity arises from the drastic changes to fuel consumption (which affects emissions) between the start and end of both the climb and descent. For instance, for the Airbus A320-200, one of the most "popular" aircrafts, its highest fuel consumption rate (kg/min) is 129.4 (at FL 0) and the lowest is 50.4 (at FL 340) (FL 1 corresponds to 100 feet of altitude).

For the descent, we observe a similar issue though on a far smaller scale. For instance, the difference between highest and lowest fuel consumption rate (kg/min) is 9.4 (at FL 0) and 5.8 (at FL 340) for the Airbus A320-200.

It is difficult to determine an average rate of fuel consumption throughout the climb/descent, as different models may be optimised to fly certain portions of the climb/descent journey at different flight levels. However, the fuel consumption (kg/min) seems to change linearly with flight level. Looking at the climb data for the Airbus A320-200, coefficient of determination $R^2 = 0.999$ and for the descent $R^2 = 0.999$ (Graphs in Appendix 4).

Therefore, per aircraft model, we measure the rate of fuel consumption (kg/min) as an average over FL 0 to FL 340. Equation 4 transforms $\frac{fuel\ (kg)}{time\ (min)}$ (averaged across relevant FL 0 and 340) into $\frac{Total\ kgCO_2e\ saved}{passenger}$ for each aircraft model.

As for cruise modelling, $\frac{Total\ kgCO_2e\ saved}{\#seats\ occupied}$ is weighted based on the aircraft model's proportion of total pkm, with plane model data from the same sources previously. A detailed derivation of the equation is in appendix 3. The metric $\frac{kg\ CO_2e\ saved}{fuel\ (kg)}$ incorporates the use of fuel cells for descent and turbines for climb.

DOI: 10.14324/111.444.2755-0877.1856

2.1.6. Modelling Emission Savings - Converting to 2050

From the above two subsections, we yield equation (5) to estimate the total emissions saved per route per passenger.

Thus with $\frac{total\ kgCO_2e\ saved}{passenger}$ fixed for climb and descent, varying with distance for the cruise phase, equation (6) estimates the total emissions saved per route.

Equation (6) applies to 2023 CO_2 e emissions (saved). We multiply it by 0.98[27] to account for efficiency improvements (2% per annum) by 2050. We multiply this emissions figure by 1.09, a correction factor used to account for circling and delays (CDF), an average across all aircraft classes and geographies globally (ICCT 2020). Furthermore, we multiply the figure by 1.019[27] to account for expected annual demand increases of 1.9% per year in Europe, averaged across all EU+ routes (NLR – Royal Netherlands Aerospace Centre and SEO Amsterdam Economics, 2021). Finally, we model each of the 3 external carbon cost scenarios to capture the uncertainty in discount rates, producing external costs of $kgCO_2e$ in 2020 euros.

Therefore, equation (7) estimates the marginal net environment benefit, as a function of ρ (discount rate) embedded in the 'Case' scenario argument.

2.2. Net Marginal Economic Cost

There are various monetary costs of our proposal. On the individual aircraft level, these costs include additional OPEX and CAPEX compared to producing and running a new kerosene-based aircraft in 2050. On the airport level, these costs include the CAPEX and OPEX related to gaseous hydrogen production, liquefaction and distribution (compared to kerosene costs). Lastly, we have a fixed R&D cost for aircraft development.

2.2.1. Aircraft OPEX and CAPEX

The OPEX of hydrogen aircrafts predominantly include maintenance, aircrew training and certification costs. According to Steer (2023), although the crew would require certification for hydrogen aircraft operation specifically, maintenance and training costs would not significantly change with the introduction of hydrogen aircraft compared to the conventional kerosene aircrafts currently.

Additionally, there is no evidence to suggest the production of new aircrafts would fundamentally incur more incremental costs. Although certain aircraft components may be cheaper or more expensive to manufacture, studies conclude that the new aircrafts' production would not carry significant production cost differences (compared to a 2050-produced kerosene-based aircraft), once the design and technology of the new aircrafts are developed. (Steer, 2023)

Therefore, we assume that there is no additional CAPEX or OPEX costs for producing each new hydrogen aircraft.

2.2.2. Airport OPEX and CAPEX - Production

The first part of the hydrogen production value chain is producing gaseous hydrogen via on-site electrolysers (Figure 5). We base the production expenditure calculations off the findings of Zhou and Searle, 2022. Their paper utilises the equivalent annual cost method (EAC) to annualise one-off CAPEX and then adds on annual OPEX (electricity, maintenance and water costs) and annual operating income (selling by-product oxygen). This is then converted into a per kg cost.

The paper's 2050 numbers are based on 2020 figures with specific growth rates applied illustrated in Figure 6. Also, we note that their paper utilises 1MW electrolyser producing 500kg of hydrogen a day. Since we require

DOI: 10.14324/111.444.2755-0877.1856

multiple (occasionally over 500) stacks for larger airports, we may utilise larger electrolysers which benefit from economies of scale. This is thus a conservative case for CAPEX and OPEX.

Furthermore, these production expenses are calculated with country level heterogeneity. These country-level differences include the price of renewable electricity, water prices and corporate tax levels (affecting the EAC's discount rate). However, the main driver for country level production OPEX differences are electricity costs.

Figure 6 (Zhou and Searle, 2022) displays the hydrogen production CAPEX and OPEX (per kg) varying by country.

2.2.3. Airport OPEX and CAPEX – Liquefaction

Since the electrolysis process produces hydrogen in gaseous form, for it to be used as fuel and to minimise the required storage space on the aircraft, it is converted to liquid through an energy-intensive liquefaction process.

The costs associated with liquefaction include CAPEX (liquefier installation) and OPEX (renewable energy to liquify it and maintenance). According to Sens et al., a hydrogen liquefier with 100 tonne/day capacity has a CAPEX of €$_{2020}$ 139M (according to the progressive case, reflecting 2050 costs). The OPEX is 4% of total CAPEX and lifespan is 30 years. Through back testing, we find the average liquefaction capacity needed for airports in our optimal subgraph would be less than 2×100 tonnes. To mitigate the complexity arising from variable marginal per-airport costs, we model each airport possessing 2 liquefaction plants of 100 tonne daily capacity, allowing for costs saved on airports requiring fewer plants to offset the need for more plants at bigger airports.

To estimate the annual cost of CAPEX, we utilise the EAC method used by Zhou and Searle, 2020, depending on the asset's useful life (n) and the discount rate given by the weighted average cost of capital (WACC), illustrated in equation (8). We further add OPEX to get the annualised total cost.

For the calculation of the WACC, we utilised the assumptions from Zhou and Searle 2020 and assume the corporate tax rate at 20.8%, as shown in figure 7.

Equation (9) utilises the assumptions to estimate the nominal WACC.

We further convert to the real WACC for use in our EAC calculations since all values have been deflated to real prices in the source. We employ equation (10) based on the Fisher equation, assuming 2% long term inflation (π):

2.2.4. Airport OPEX and CAPEX - Distribution

According to Steer, the distribution-related CAPEX arises from constructing/changing airport infrastructure such as storage and transport from on-site electrolyser to aircrafts (via pipeline or bowsers). The main OPEX is the renewable energy required to store liquified hydrogen at cryogenic temperatures. We note that storage facilities will be required to handle four times the volume of fuel compared to current amounts of kerosene, because of volumetric energy density differences, which may potentially lead to more hours of fuelling time compared to present day. As part of our investigation, we have assumed that there are no constraints on an airports' ability to construct hydrogen infrastructure (e.g. land, maximum electricity available from the grid). We also disregard potential additional costs such as the extension of airport gate sizes, as hydrogen aircrafts are likely to be longer in length than present-day aircrafts to house more voluminous fuel.

Steer (2023) quotes that across Europe's 100 most popular airports, a total CAPEX of €$_{2020}$ 27.6B is required. In reality, the CAPEX will vary depending on the size of the airport and the storage capacity required. Moreover, the infrastructure in Steer's paper is built over a 20-year period (2030-2050). We thus disregard the pricing differences across time (due to inflation and technological development) and calculate the CAPEX for a "representative" popular airport, which is estimated at €$_{2020}$ 27.6B/100 = €$_{2020}$ 276M. The useful life is 30 years and the real WACC

DOI: 10.14324/111.444.2755-0877.1856

will be identical for the liquefaction case. We further add OPEX to annualised CAPEX to calculate total annualised cost.

2.2.5. Aircraft Development Costs

According to Steer, aircraft R&D costs are assumed at €$_{2020}$ 15 billion over a 10-year period. We apportion these development costs over the same 30-year period as before using the EAC method with the same real WACC from previous sections.

2.2.5. Private Net Cost of Fuel

Calculating the marginal costs of switching from kerosene to liquid hydrogen requires factoring in the kerosene costs as well. For simplicity and due to the lack of available aircraft in operation, we approximate the difference in fuel intensities by the fuels' respective gravimetric energy densities as in section 1. We also assume that efficiency improvements apply equally between the aircrafts - a conservative case given that kerosene engines are more established.

Kerosene prices have risen significantly relative to inflation since 2000 based on US figures (US Energy Information Agency, 2024) (Our World in Data, 2024). Since we couldn't obtain relevant kerosene prices over time, we derived a 'real, long-run' growth rate of kerosene prices based on the above sources and applied it to current EU+ kerosene prices as per International Air Transport Association (2023) (obtaining 4.28% annual growth). Furthermore, we also consider the case where a €0.55 tax per litre of kerosene is applied, since aviation kerosene is still tax-exempt in the EU (Schulz, 2019). Hemmings et al. (2020) concluded €0.55 per litre represents the optimal level of a single fuel tax, assuming the external cost of carbon is set at $80 per tonne of CO_2. This optimal rate is determined to be able to address the environmental externalities from aviation and simultaneously raise tax revenue, amounting to €26-€49 billion annually within EU+. We further assume a 1.3% growth in flight counts in EU+ as per (NLR – Royal Netherlands Aerospace Centre and SEO Amsterdam Economics, 2021), giving a 1.013[31] scaling factor (τ). Modelling this with hydrogen costs from Figure 6 and variables defined previously in section 2.1, equation (11) estimates the private net fuel cost.

2.3. EU + Airport Network Model

2.3.1. Airport Network Data

To conduct the network analysis and form the graphics that we use, we employ four sets of data:

(1) Coordinates and names of EU+ airports with relevant data
(2) Passenger count for routes within EU+ in 2019 (1
(3) Flight count for routes within EU+ in 2019
(4) Predicted cost of hydrogen in 2050

Finally, we produce a 345×345 matrix (where 345 is the number of airports modelled) with a 6-item vector at each element containing:

1. Distance between the two airports
2. Average hydrogen cost predicted at 2050 for the two airports
3. Number of flights between the airports in 2019
4. Number of passengers between the airports in 2019
5. Name of first airport
6. Name of second airport

We use a distance matrix made by the European Commission (EC) (GISCO, n.d.) and further trace the source of the coordinates the EC used to ourairports.com (Our Airports, 2024). Index matching is used to find the coordinates

DOI: 10.14324/111.444.2755-0877.1856

of all airports with both flight and passenger data available. Through sorting by latitude and longitude respectively and plotting in Wolfram Mathematica, anomalous results and European territories in other continents were removed from the dataset. Wolfram Mathematica is further used to create a customised distance matrix through the GeoDistance command which calculates geographical distances.

Average hydrogen cost values for 2050 (Zhou and Searle, 2022) from section 2.2 are used and mean values are used for any country which is not in the dataset. It is assumed that all airports within that country face the same costs of hydrogen.

Annual passenger and flight count data are found from the Eurostat database (Eurostat, 2022) and is compiled using Microsoft Excel. Missing values, duplicated routes, and routes outside of EU+ are cleaned using Python.

2.3.2. Welfare Network & Optimisation

After obtaining the heterogeneous data, we combine the information to produce a network graph G with (1) each link weight denoting the marginal benefit decarbonising route ij, in PV terms and (2) each node representing an airport, which, if decarbonised, would incur a homogenous fixed cost.

Using the earlier data and equations, equation (12) estimates the marginal benefit of route (MBR).

We model both airports i and j needing an electrolysis plant in our model for the link ij to be considered 'decarbonised' and thus for the MBR to be extracted. This problem is thus a combinatorial optimisation task, which we call ‘Welfare Maximisation’, defined as:

Definition 1 (WM): *Given a graph G=(V,E), find a (not necessarily connected) subgraph G'=(V',E') where V' ⊆ V, E' ⊆ E that maximises:*

$$\mathrm{WM}(G') = \sum_{e \in E'} p(e) - \sum_{v \in V'} c(v)$$

Where p(e) denotes MBR of edge e and c(v) denotes the cost of vertex c (in our case, c(v)=C is fixed)
This problem may seem similar to the Net-Worth Maximisation Problem, a variant of the Price-Collecting Steiner Tree (PCST) Problem (Johnson et al. 2000). This variant requires a subtree T' that maximises:

$$\mathrm{NW}(T') = \sum_{v \in V'} p(v) - \sum_{e \in E'} c(e)$$

Although seemingly an inversion of our problem, we could not find research tackling WM and struggled to generalise existing solutions to NW due to the constraint that edge costs and node profits must be non-negative (Johnson et al. 2000). Instead, we propose a novel hypothetical solution and a family of approximation algorithms, WMx.
First, a hypothetical algorithm to solve (our case of) WM:

(1) Set the original graph G of size N to be the active subgraph Ga (whose size we denote as Na).
(2) Compute weighted degree centralities of all nodes in Ga.
(3) What we call ‘1st-order pruning' would first consider eliminating nodes from Ga one at a time: the algorithm finds the node with the lowest degree centrality and, if this measure is < C, then it would necessarily be optimal to prune this node (since its marginal benefit, captured by degree centrality, is less than marginal cost, C), after which the weighted degree centralities would be re-calculated on the remaining Ga.
(4) Iterate step (3) until the next ‘worst’ node is not worth getting rid of, i.e. its sum of degrees > C.
(5) Proceed to 2nd-order pruning and consider two nodes at a time. An Na-by-Na matrix is formed, with each element *ij* denoting the sum of degrees of nodes *i* and *j* (without overlap) that would be eliminated should both nodes *i* and *j* be pruned simultaneously. The algorithm then chooses the smallest element in this matrix, and if this value is < 2C, then nodes *i* and *j* are pruned

DOI: 10.14324/111.444.2755-0877.1856

(6) Iterate steps (3-5), since now there may be single nodes worth pruning due to the heterogenous update to degree centralities until the next 'worst' two-node combination is not worth pruning, i.e. its sum of degrees > 2C.
(7) Proceed to Kth -order pruning, generalising the logic in steps (5-6) by forming K-dimensional matrix, evaluating against < K C, and iterating all previous steps from (3).
(8) Stop pruning and return active subgraph Ga once K=Na -order pruning finds no more K-node combinations of nodes worth eliminating.

This approach is clearly computational prohibitive without an approximation algorithm: for instance, a 300×300 graph may need a matrix with 300^{300} elements, equivalent to a $10^{371}\times10^{371}$ matrix, for 300th-order pruning. Therefore, we present 3 approximation algorithms with increasing optimality: WMx1, WMx2, and WMx3, beyond which our resources are limited to calculate exact solutions. We compare these with the null case (0) where *all* airports are decarbonised and 2 heuristic algorithms (A) and (B) as potential candidates to approximately solve WM:

(A) Calculates weighted degree centralities of G and prunes nodes whose sum of degree < C to return G'.
(B) Involves the following algorithmic steps:

(5) Set Ga = G.
(6) Calculate and save total welfare of current Ga (at step t).
(7) Calculate eigenvector centralities of nodes remaining in Ga.
(8) Prune the node with lowest eigenvector centrality based on updated rankings in (3) (irrespective of whether this step is marginally beneficial).
(9) Iterate steps (1-3) until no nodes are left and obtain *t=OptimalTime* when Ga's welfare is greatest.
(10) Run the iteration again but only up until *OptimalTime* inclusive to return G'=Ga.

All algorithms select the null graph as G' if their optimal matrix produces negative welfare.
By comparing the above candidates for the best optimisation algorithm on a sample of 200 toy random graphs, we gain insight about which method may yield the optimal decarbonised sub-network of airports from the MBR-weighted EU+ airport network.

3. Modelling

3.1. Environmental Benefit Analysis

Under the estimations set out in section 2.1.3 from Lee et at. (2021) and (GWP NO_x) source, figure 8a illustrates our estimates for the (kg CO_2e/kg kerosene) for each individual emissions, providing a benchmark to compare the impact of various emissions for both kerosene and hydrogen planes.

Figure 8b shows the changes in emission statistics should we choose to use fuel cells or turbines, holding the same energy output potential if from kerosene.

Thus, when we operate H_2 fuel cells instead of kerosene aircrafts, we save 4.59 (5.4-0.78) kg CO_2e per kg kerosene that would have otherwise been combusted. When we operate H_2 turbines instead of kerosene aircrafts, we save 3.86 (5.4-1.51) kg CO_2e per kg kerosene that would have otherwise been combusted.

3.1.1. Identifying Emissions Saved during Cruise

To identify the most popular aircrafts, we utilise the proportion of total pkm. GHG 2023 lists 31 aircrafts, although 18 of them have "0%" of proportion of passenger km written, as the percentages are rounded to the nearest digit. Resultantly, the sum of the total percentages of proportion of passenger km is 98%, with 18 negligible aircrafts adding up to 2%. We use 98% as the sum of the weightings, based on the proportion of total passenger kilometre.

DOI: 10.14324/111.444.2755-0877.1856

We estimate the weighted average at 0.08 kg CO_2e saved per passenger kilometre, with the full derivation in the appendix 5.

Using the methodology from section 2.1.6, we estimate the weighted average of horizontal distance for climb and descent at 280 km and 281 km respectively, with the full derivation in the appendix 5.

Equation (13) illustrates the input of our estimated values into equation (3) from the methodology.

3.1.2. Identifying Emissions Saved during Climb and Descent

Using the methodology from section 2.1.7, we estimate the weighted average of the total $kgCO_2$ saved per passenger for climb and descent at 43.15 kg and 4.87 kg respectively.

3.1.3. Calculating Raw Total Emissions Saved

Equation (14) utilises our estimates for emissions saved to compute the total emissions saved. Equation (15) converts this to the social cost of total emissions in 2050, with the circling and delays factor (CDF) at 1.09, compounded growth of demand (η) at 1.66 and compounded growth of efficiency improvement (μ) at 0.58.

3.2 Economic Cost Analysis

3.2.1. Production

Production is directly taken from Steer (2024) p.20-21, integrating country level heterogeneity.

3.2.2. Liquefaction

Given the assumptions set out in the methodology including the cost of debt and equity, the nominal WACC is estimated at 8.3% and the real WACC at 6.18%. We note the conservative nature of the WACC adopted, as other papers such as Steer use a lower cost of equity and debt (14% and 2% respectively), which would produce a higher EAC value.

Thus, the EAC of CAPEX is €$_{2020}$ 20.6M. Adding the OPEX of €$_{2020}$ 11.2M (4% of 139 x 2), the total annual cost per liquefaction plant is €$_{2020}$ 31.8M for 2 x 100 tonnes/day hydrogen capacity.

3.2.3. Distribution

Using the methodology from section 2.2.4, EAC is €$_{2020}$ 20.4M. The OPEX is quoted at 4.7% (€$_{2020}$ 12.97M) and thus the annual cost of airport infrastructure is €$_{2020}$ 33.37M.

3.2.4. R&D

Using the methodology from section 2.2.5, this yields an annual lump-sum cost of €$_{2020}$ 1.11B into R&D.

3.2.5. Private Net Fuel Costs

Applying methods from section 2.2.6, equation (16) calculates private fuel costs (hydrogen less kerosene) for a given flight route.

3.2.5. Total Cost

DOI: 10.14324/111.444.2755-0877.1856

Depending on distance and flight count of the route that gets decarbonised, private net fuel costs are calculated as per equation above. For every airport decarbonised, the per-airport costs modelled are for the duration of 30 years, €$_{2020}$ 31.8M annually for liquefaction and €$_{2020}$ 33.37M annually for distribution. Regardless of the routes decarbonised, R&D fixed costs amount to €$_{2020}$ 1.11B annually.

3.3 Airport Network Modelling

3.3.1. Welfare Maximisation Algorithms

First, we compare potential optimisation algorithms for WM. We find that each higher-order version of WMx algorithm weakly outperforms the previous in all toy-model cases within a sample size of 200, and WMx3 outperforms both (A), (B), and (0).

3.3.2. Decarbonisation Scenarios

Having demonstrated successful performance of WMx3, we apply it to our MBR network, obtaining the optimal decarbonisation sub-network for each of the progressive, central, and conservative scenarios, without and with the €20200.55/litre kerosene tax respectively. Summary variables surrounding the welfare and environmental impact (during 2050 in €2020 terms) for each of these 6 sub-networks are presented in Figure 11 and visualised in Figure 12. Finally, we visualise the set of routes decarbonised in Figure 13 – which juxtaposes our most contrasting scenarios – and use Figure 14 to illustrate differences in airports decarbonised between scenarios.

3.3.3. Sub-network Analysis

To understand the factors driving our algorithm's choice of the optimal sub-graph of airports to decarbonise, we compare 4 graph properties of each scenario against the full airport network. These factors, presented in Figure 15, capture (1) route popularity, (2) hydrogen cost, (3) airport clustering, and (4) route distance respectively. These factors are also visualised in Figure 16. We also note positive correlation of 0.1398 between average passenger degree and H2 costs, which may explain the higher hydrogen cost in the selected sub-network.

4. Discussion & Conclusion

4.1 Discussion of Results

Our welfare optimisation algorithm successfully obtained sub-networks of airports to decarbonise which, under each of the 6 scenarios tested, generated billions of euros in long-run annual welfare (Figure 11). The central case (3% discount rate for external cost of carbon dioxide) under no additional policy is expected to yield €2.79bn annually in aggregate welfare during 2050, represented in 2020 euros, with this value ranging from €3.58-0.89bn by scenario.

It is worth noting that this welfare gain is specific to 2050 and will change year to year due to demand growth and efficiency growth affecting marginal benefit and marginal costs. However, the increase in marginal benefit should exceed marginal cost and thus we conservatively deem the welfare gain of €2.79bn as "annual" (up until an increase in fixed costs is needed to adjust for increased demand, far into the future, beyond our scope).

Intuitively, an increase in the discount rate causes a fall in the external cost of carbon, prompting a drop in welfare gain and the number of airports decarbonised. Similarly, implementing a kerosene tax reduces the cost of switching routes to hydrogen, allowing more airports to be worth decarbonising. In the central case, this is expected to increase long-run annual welfare gained by 112% compared to without the tax, yielding an additional €20203.13bn of welfare annually. Our model also shows that the optimal selection of airports, under any scenario, has at least 25% of main EU+ airports equipped with hydrogen infrastructure in the long run. Overall, these results highlight the large economic significance and opportunity for hydrogen technology to be used in short-haul commercial aviation in EU+.

DOI: 10.14324/111.444.2755-0877.1856

Figures 9 and 10 highlight the validity of our optimisation algorithm. Intuitively, successive orders of WMx prune the same or more nodes than the previous order, but since these (multi-node) prunes are necessarily beneficial, a higher-order WMx always weakly outperforms the previous. This is also why any WMx algorithm outperforms (A). Figure 9 also shows that there may be 'diminishing marginal returns' to higher orders of WMx, suggesting that our solution derived via WMx3 is indeed a suitable approximation to the WM problem.

Seeking to understand our algorithm's choice of the optimal sub-network of airports to decarbonise, we learn from Figure 15 that:

(1) Airports with greater passenger count degree (i.e. more 'popular' airports) are more likely to be worth decarbonising
(2) Counterintuitively, hydrogen costs are higher at airports chosen for decarbonisation, likely due to the positive correlation between hydrogen costs and airport popularity
(3) The decarbonised network is over twice more highly clustered than the original, taking advantage of positive network effects
(4) Shorter routes are prioritised, likely because of their higher pollutive capability per km

These results highlight the nuance within our network modelling, showing how multiple economic and environmental factors are successfully integrated into our choice of airports to decarbonise.

4.2 Assumptions and Limitations

Analysing aircrafts' environmental impact, we assume constant GWP100 values. As greenhouse gases remain in the atmosphere for extended periods of time and thus have a cumulative effect, our assumption of constant values may be inaccurate. Moreover, our conversion of engine efficiency between kerosene and hydrogen is based on gravimetric energy density alone.

Our analysis is based on representative aircrafts and representative airports for liquefaction and distribution. For the aircrafts, it is based on the UK's fleet rather than European fleets and thus it may not be entirely representative, especially as the UK is one of the wealthier EU+ countries and may have a more modern fleet. We highlight this as a limitation since it suggests our results could be an over-estimate. Hence, further research, co-led by aircraft engineers/researchers, would be necessary to form policy.

For modelling climb and descent, we assume constant time to climb/descent and planes climb/descend at a constant angle. In practice, different aircraft models have varying trajectories and fly different parts of the climb and descent at different speeds. Furthermore, different aircrafts are optimised to travel phases of climb and descent at different speeds which may lead to significant contrasts in fuel consumption.

Several simplifications have been made surrounding airport infrastructure costs. For instance, slower refuelling may increase aircraft turnaround time, reducing flight count and revenues. Gate sizes may also need to be changed, increasing costs. Our estimation of EAC is also highly dependent on our assumptions such as cost of equity and debt, which are based solely on the ICCT report. We also assume various growth rates as constant such as 2% efficiency improvements and flight count increasing by 1.3%. Additionally, the fast-growing and innovative nature of the hydrogen sector results in difficulties in cost prediction and therefore our research presents only a guideline. Furthermore, given the paper's focus on long-run restricts potential implications, including the timeline to which airports to decarbonise first. We also do not consider the varying costs over time and that significant share of CAPEX and R&D must be done 5-10 years before the route is fully decarbonised.

Our model assumes continuous, uniform air traffic. However, certain airports may be highly seasonal or display any other periodic pattern such as being busier during weekends, then traffic may increase beyond the capacity of hydrogen production, thus making the predicted costs not viable. We also assume full decarbonisation of each hub for it to be included. However, in reality it may be more effective to only decarbonise flight routes partially at certain hubs. Furthermore, although we aim to capture the full welfare implications, our study simplifies welfare analysis by

DOI: 10.14324/111.444.2755-0877.1856

assuming the region internalises all "global" environmental impact. Thus, we do not model the distribution of welfare changes (such as between producers and consumers), and only consider aggregate impacts. when evaluating the welfare impact under the kerosene tax, we assume any tax revenues generated perfectly offset the consumer/producer surplus lost due to higher flight prices for polluting aviation.

The original flight and passenger count data used in modelling may be incomplete and contains some erroneous values which are removed. Differences are also observed in reporting of the same route from the two different airports on the route; mean values are taken. Additionally, the values for hydrogen cost are absent for some countries due to different datasets used. Again, we take a mean value to fill these.

To model our problem in the form of WM, we restricted complexity by modelling many airport costs as homogenous. Our solution is also limited by expertise in com¬¬¬¬binatorial optimisation and computational constraints. For instance, despite successful sample testing, our toy models have a lower network density than our real model (0.102 vs 0.155 respectively): we struggle to see noticeable outperformance for toy graphs of density 0.155, potentially due to low pruning order in our WMx¬ algorithms. Nonetheless, since our model illustrates that billions in welfare can be unlocked, we hope to inspire future research to optimise the modelling further.

Finally, our analysis only considers 2050: it may be that in the years after, demand and/or cost patterns shift, making the welfare trade-off no longer marginally beneficial for some routes. Nonetheless, sunk infrastructure costs would've already been implemented, hence hydrogen flights may remain as the Nash equilibrium.

4.3 Policy Suggestions

Beyond taxation, other possible policy would be green hydrogen tax credits. These act similarly to a subsidy and have already been utilised in the US. In 2022, the Inflation Reduction Act (IRA) was passed, where clean hydrogen plants producing hydrogen by using less than 0.45kg of CO2e per kg of H2 will get a $3/kg tax credit for the next 10 years. For more pollutive hydrogen, producers will receive a fraction of the $3/kg tax credit (ranging from $1/kg to $0.45/kg) (Collins, 2021). This policy's total size is expected to be $137 billion over the next 10 years (BloombergNEF, 2023). Moreover, this tax credit acts as a "direct pay", as clean hydrogen producers can claim a tax refund equal in value to their tax credits for five years. Additionally, producers can benefit from tax "transferability" - the ability to sell the credit between producers.

In the EU, similar funding mechanisms have been put in place. In November 2023, the European Hydrogen Bank auction was announced, where producers can bid for €800 million worth of emissions trading revenues, channelled through the Innovation Fund, in the form of fixed premium per kilogram of hydrogen produced (European Commission, 2023a). Additionally, the EU is also offering an additional auctions-as-a-service mechanism, where member states can support projects which bid for the EU Hydrogen Bank funding but didn't receive it due to budget limitations (European Commission, 2023a).

All these funding mechanisms help bring production to scale, bridge the price gap between producers and consumers, and stimulate investment. All of this is crucial to ensure consumer welfare is not harmed by the costly shift to hydrogen. Moreover, the US subsidies can be financed by kerosene taxes whilst the EU subsidies are financed by selling EU Emissions Trading Systems allowances, and thus the government's fiscal burden should be limited (European Commission 2023b).

No matter the policy type, international collaboration between European nations is crucial. Therefore, EU-wide legislation should be introduced to unify standards and regulations for the adoption of hydrogen in commercial aviation and the taxation of kerosene. CORSIA (Carbon Offsetting and Reduction Scheme for International Aviation) is an example of such an alliance where over 160 countries globally agreed to keep CO2 emissions below the 2020 level (ICAO, 2019). This collaboration not only is key to preventing the tragedy of the commons, but will also lead to faster innovation, greater economies of scale, greater incentives to invest, and a level playing field, so that benefits are shared all across society (IEA, 2022).

DOI: 10.14324/111.444.2755-0877.1856

References

Alternative Fuels Data Center. (n.d.). Alternative Fuels Data Center: Fuel Cell Electric Vehicles. [online] Available at: https://afdc.energy.gov/vehicles/fuel_cell.html#:~:text=The%20electrons%20are%20forced%20to.

Anderson, K. (2023). Short-haul flights: Is France's ban a good way to cut emissions? [online] greenly.earth. Available at: https://greenly.earth/en-gb/blog/ecology-news/short-haul-flights-is-frances-ban-a-good-way-to-cut-emissions.

BloombergNEF. (2023). Hydrogen Subsidies Skyrocket to $280 Billion With US in the Lead. [online] Available at: https://about.bnef.com/blog/hydrogen-subsidies-skyrocket-to-280-billion-with-us-in-the-lead/ [Accessed 5 Jan. 2024].

Bond, T. C. (2013).Bounding the role of black carbon in the climate system: A scientificassessment. JGR Atmospheres.

Brown, R. C.(1996). Aircraft exhaust sulfur emissions. Geophysical Research Letters.

Burkhardt, U.,& Kärcher, B. (2011). Global radiative forcing from contrail cirrus. NatureClimate Change, 54-58.

Business Insider (2023). Crude oil price. [online] markets.businessinsider.com. Available at: https://markets.businessinsider.com/commodities/oil-price.

CAPA (2021). Aviation industry glossary | CAPA. [online] centreforaviation.com. Available at: https://centreforaviation.com/about/glossary Short Haul.

Collins , L. (2021). New clean hydrogen production tax credit of up to $3/kg approved by US House, paving way for cheap green H2 | Recharge. [online] Recharge. Available at: https://www.rechargenews.com/energy-transition/new-clean-hydrogen-production-tax-credit-of-up-to-3-kg-approved-by-us-house-paving-way-for-cheap-green-h2/2-1-1102245 [Accessed 5 Jan. 2024].

Environmental Protection Agency (2023). Supplementary Material for the Regulatory Impact Analysis for the Supplemental Proposed Rulemaking, 'Standards of Performance for New, Reconstructed, and Modified Sources and Emissions Guidelines for Existing Sources: Oil and Natural Gas Sector Climate Review' EPA External Review Draft of Report on the Social Cost of Greenhouse Gases: Estimates Incorporating Recent Scientific Advances. [online] Available at: https://nepis.epa.gov/Exe/ZyNET.exe/P1018BVI.TXT?ZyActionD=ZyDocument&Client=EPA&Index=2016+Thru+2020&Docs=&Query=&Time=&EndTime=&SearchMethod=1&TocRestrict=n&Toc=&TocEntry=&QField=&QFieldYear=&QFieldMonth=&QFieldDay=&IntQFieldOp=0&ExtQFieldOp=0&XmlQuery=&File=D%3A%5Czyfiles%5CIndex%20Data%5C16thru20%5CTxt%5C00000036%5CP1018BVI.txt&User=ANONYMOUS&Password=anonymous&SortMethod=h%7C-&MaximumDocuments=1&FuzzyDegree=0&ImageQuality=r75g8/r75g8/x150y150g16/i425&Display=hpfr&DefSeekPage=x&SearchBack=ZyActionL&Back=ZyActionS&BackDesc=Results%20page&MaximumPages=1&ZyEntry=1&SeekPage=x&ZyPURL [Accessed 5 Jan. 2024].

Eurocontrol Experimental Centre. (1998). Base of Aircraft Data (BADA) Revision 3.0. Available at: https://www.eurocontrol.int/node/10065

European Commission (2023a). Commission launches first European Hydrogen Bank auction with €800 million of subsidies for renewable hydrogen production. [online] European Commission. Available at: https://ec.europa.eu/commission/presscorner/detail/en/ip_23_5982.

European Commission (2023b). EU Emissions Trading System (EU ETS). [online] European Commission. Available at: https://climate.ec.europa.eu/eu-action/eu-emissions-trading-system-eu-ets_en.

Eurostat. (2022). Available at: https://ec.europa.eu/eurostat/databrowser/explore/all/all_themes?lang=en&display=list&sort=category.

European Environment Agency (2023). Transport and mobility. [online] www.eea.europa.eu. Available at: https://www.eea.europa.eu/en/topics/in-depth/transport-and-mobility?activeTab=fa515f0c-9ab0-493c-b4cd-58a32dfaae0a.

European Union (2021a). EUR-Lex - 32021R1119 - EN - EUR-Lex. [online] Europa.eu. Available at: https://eur-lex.europa.eu/legal-content/EN/TXT/?uri=CELEX:32021R1119 Article 2.

European Union (2021b). EUR-Lex - 32021R1119 - EN - EUR-Lex. [online] Europa.eu. Available at: https://eur-lex.europa.eu/legal-content/EN/TXT/?uri=CELEX:32021R1119 Article 4.

Exchange Rates UK. (2020). US Dollar to Euro Spot Exchange Rates for 2020. [online] Available at: https://www.exchangerates.org.uk/USD-EUR-spot-exchange-rates-history-2020.html#:~:text=This%20is%20the%20US%20Dollar [Accessed 4 Jan. 2024].

DOI: 10.14324/111.444.2755-0877.1856

Fuel Cells and Joint (2020). Hydrogen-powered aviation: a fact based study of hydrogen technology, economics, and climate impact by 2050. [online] Publications Office of the European Union. Publications Office of the European Union. Available at: https://data.europa.eu/doi/10.2843/471510.

Gisco. (n.d.). TERCET. [online] Available at: https://gisco-services.ec.europa.eu/tercet/flat-files [Accessed 6 Jan. 2024].

Givoni, M. and Rietveld, P. (2010). The environmental implications of airlines' choice of aircraft size. Journal of Air Transport Management, [online] 16(3), pp.159–167. doi:https://doi.org/10.1016/j.jairtraman.2009.07.010.

Groningen Airport Eelde. (2023). Unveiling electrolyser to produce green hydrogen at Groningen Airport Eelde. [online] Available at: https://www.groningenairport.nl/en/news/unveiling-electrolyser-to-produce-green-hydrogen-at-groningen-airport-eelde [Accessed 6 Jan. 2024].

Harper, S., Lam, S. and Dodd, W. (2021). COP26: How the world will measure progress on the Paris climate agreement and keep countries accountable. [online] The Conversation. Available at: https://theconversation.com/cop26-how-the-world-will-measure-progress-on-the-paris-climate-agreement-and-keep-countries-accountable-160325.

Hemmings, B., Pache, E., Forsyth, P., Mundaca, G., Strand, J. and Kågeson, P. (2020). Taxing Aviation Fuel in Europe. Back to the Future? Report prepared by Bill Hemmings and expert contributors. [online] Available at: https://www.transportenvironment.org/wp-content/uploads/2021/07/2020_06_Study_for_TE_Taxing_aviation_fuel_final.PDF [Accessed 5 Jan. 2024].

Hydrogen-powered aviation. (2020). Available at: https://www.euractiv.com/wp-content/uploads/sites/2/2020/06/20200507_Hydrogen-Powered-Aviation-report_FINAL-web-ID-8706035.pdf.

IATA (2021). Our commitment to fly net zero by 2050. [online] www.iata.org. Available at: https://www.iata.org/en/programs/environment/flynetzero/.

ICAO (2019). Carbon Offsetting and Reduction Scheme for International Aviation (CORSIA). [online] Icao.int. Available at: https://www.icao.int/environmental-protection/CORSIA/Pages/default.aspx.

IEA, IRENA & UN Climate Change High-Level Champions (2022), Breakthrough Agenda Report 2022, IEA, Paris https://www.iea.org/reports/breakthrough-agenda-report-2022, License: CC BY 4.0

IER (2023). EPA Ups Estimates for the Social Cost of Carbon. [online] IER. Available at: https://www.instituteforenergyresearch.org/regulation/epa-ups-estimates-for-the-social-cost-of-carbon/ [Accessed 5 Jan. 2024].

Interagency Working Group on Social Cost of Greenhouse Gases, United States Government (2021). Social Cost of Carbon, Methane, and Nitrous Oxide Interim Estimates under Executive Order 13990 Interagency Working Group on Social Cost of Greenhouse Gases, United States Government With participation by. [online] Available at: https://www.whitehouse.gov/wp-content/uploads/2021/02/TechnicalSupportDocument_SocialCostofCarbonMethaneNitrousOxide.pdf.

International Air Transport Association (2023). Jet Fuel Price Monitor. [online] IATA. Available at: https://www.iata.org/en/publications/economics/fuel-monitor/.

IPCC. (1999). Aviation and the Global Atmosphere. Cambridge University Press.

Johnston, M. (2023). How High Do Commercial Planes Fly? [online] CAU. Available at: https://calaero.edu/how-high-do-commercial-planes-fly/ [Accessed 5 Jan. 2024].

Lee, D. (2021). The contribution of global aviation to anthropogenic climate forcing for 2000 to2018. Atmospheric Environment.

Lee, D. S. (2018). The current state of scientific understanding of the non-CO2 effects of aviaton on climate. Manchester: Manchester Metropolitan University.

Masterson, V. (2022). The European Union has cut greenhouse gas emissions in every sector - except this one. [online] World Economic Forum. Available at: https://www.weforum.org/agenda/2022/09/eu-greenhouse-gas-emissions-transport/.

Meerkoetter, R.(1999). Radiative forcing by contrails. Ann. Geophysicae.

Nations, U. (2015). Paris agreement. [online] Available at: https://unfccc.int/sites/default/files/english_paris_agreement.pdf Article 2.

NLR – Royal Netherlands Aerospace Centre and SEO Amsterdam Economics (2021). Home. [online] https://www.destination2050.eu/. Available at: https://www.destination2050.eu/.

Our World in Data. (2024). Consumer price index. [online] Available at: https://ourworldindata.org/grapher/consumer-price-index?time=2000..latest [Accessed 6 Jan. 2024].

Our Airports. (2024). Map of airports in Europe @ OurAirports. [online] Available at: https://ourairports.com/continents/EU/ [Accessed 6 Jan. 2024].

Schulz, F. (2019). Why we are far from imposing a tax on kerosene. [online] www.euractiv.com. Available at: https://www.euractiv.com/section/aviation/news/why-we-are-far-from-imposing-a-tax-on-kerosene/.

Shell (n.d.). Decarbonising aviation. [online] www.shell.com. Available at: https://www.shell.com/energy-and-innovation/the-energy-future/decarbonising-aviation.html.

Skowron, A., Lee, D.S. and De León, R.R. (2015). Variation of radiative forcings and global warming potentials from regional aviation NO x emissions. Atmospheric Environment, 104, pp.69–78. doi:https://doi.org/10.1016/j.atmosenv.2014.12.043.

Steer (2023). Analysing the Costs of Hydrogen Aircraft. [online] Belgium: Transport & Environment. Available at: https://www.transportenvironment.org/wp-content/uploads/2023/05/Study-Analysing-the-costs-of-hydrogen-aircraft.pdf [Accessed 5 Jan. 2024].

Transport and Environment (2024). Airplane pollution. [online] Campaigning for cleaner transport in Europe | Transport & Environment. Available at: https://www.transportenvironment.org/challenges/planes/airplane-pollution/.

World Meteorological Organization. (2023). 2023 shatters climate records, with major impacts. [online] Available at: https://wmo.int/news/media-centre/2023-shatters-climate-records-major-impacts#:~:text=Temperatures%20in%20Italy%20reached%2048.2 [Accessed Jan. 2024].

Wu, T.L. (2022). Examining the pros and cons of hydrogen energy. [online] Earth.org. Available at: https://earth.org/pros-and-cons-of-hydrogen-energy/.

US Energy Information Agency. (2024). U.S. Gulf Coast Kerosene-Type Jet Fuel Spot Price FOB (Dollars per Gallon). [online] Available at: https://www.eia.gov/dnav/pet/hist/eer_epjk_pf4_rgc_dpgA.htm.

Zhou, Y. and Searle, S. (2022). Cost of renewable hydrogen produced onsite at hydrogen refueling stations in Europe. [online] International Council on Clean Transportation. Available at: https://theicct.org/publication/fuels-eu-onsite-hydro-cost-feb22/ [Accessed 5 Jan. 2024].

DOI: 10.14324/111.444.2755-0877.1856

Appendix 1: Equations

Equation (1)

$$\frac{kgCO_2e\ saved}{km \times \#\ seats\ occupied} = \frac{fuel\,(kg)}{time\,(min)} \times \frac{1}{speed\,(\%\ Mach)} \times \frac{Mach}{km/min} \times \frac{1}{\#\ seats\ available} \times \frac{\#\ seats\ available}{\#\ seats\ occupied} \times \frac{kgCO_2e\ saved\ (fuel\ cells)}{fuel\ (kg)}$$

Where $\frac{\#\ seats\ available}{\#\ seats\ occupied} = \frac{1}{Load\ Factor}, \frac{Mach}{km/min} = 20.58$

Equation (2)

$$Horizontal\ Distance^2 = (Speed \times Time\ to\ Climb)^2 - 10.36^2$$

Equation (3)

$$\frac{total\ kgCO_2e\ saved_{(cruise)}}{passenger} = (Total\ Distance - Horizontal\ Climb - Horizontal\ Descent) \times \frac{kgCO_2e\ saved_{cruise}}{passenger\ km}$$

where passenger refers to actual seat occupied.

Equation (4)

$$\frac{Total\ kg\ CO_2e\ saved}{\#\ seats\ occupied} = \frac{fuel\ (kg)}{time\ (min)} \times \frac{1}{\#\ seats\ available} \times \frac{\#\ seats\ available}{\#\ seats\ occupied} \times \frac{kg\ CO_2e\ saved}{fuel\ (kg)} \times t$$

where t denotes total travel time.

Equation (5)

$$\frac{kgCO_2e\ saved_{(route)}}{passenger} = \frac{total\ kgCO_2e\ saved_{(climb)}}{passenger} + \frac{total\ kgCO_2e\ saved_{(descent)}}{passenger} + \frac{total\ kgCO_2e\ saved_{(cruise)}}{passenger}$$

Equation (6)

$$total\ kgCO_2e\ saved_{(per\ route)} = \frac{kgCO_2e\ saved_{(route)}}{passenger} \times total\ passengers$$

DOI: 10.14324/111.444.2755-0877.1856

Equation (7)

$$Marginal\ Net\ Environmental\ Benefit = Total\ kgCO_2e\ saved \times External\ Carbon\ Cost\ [Case] \times CDF \times \eta \times \mu$$

where CDF refers to the circling and delays factor, η refers to the compound demand increase and μ refers to the compound efficiency improvement.

Equation (8)

$$EAC = \frac{(Asset\ Value \times WACC)}{1 - (1 + WACC)^{-n}}$$

Equation (9)

$$Nominal\ WACC = 60\% \times Rd \times (1 - t) + 40\% \times Re$$

Equation (10)

$$Real\ WACC = \frac{1 + Nominal\ WACC}{1 + \pi} - 1$$

Equation (11)

$$Private\ Net\ Fuel\ Cost = Hydrogen\ Cost\ €/Year - Kerosene\ cost\ €/Year$$

$$= \left(\frac{H_2\ €/Kg\ Airport\ i + H_2\ €/Kg\ Airport\ j}{2} \times \frac{GED_{Kerosene}}{GED_{Hydrogen}} - Kerosene\ Cost\ €/kg\ [TaxQ] \right)$$

$$\times Piecewise(Fuel\ Intensity\ Kg/min \times Distance\ km \times Speed^{-1}\ min/km) \times CDF$$
$$\times Route's\ Annual\ Flight\ Count \times \mu \times \tau$$

where μ refers to the compound efficiency improvement, τ refers to the compounded growth of flight count in EU+ and GED_i denotes the gravimetric energy density of i.

Equation (12)

$$MBR_{ij} = Marginal\ Net\ Environmental\ Benefit_{ij} - Marginal\ Net\ Economic\ Cost_{ij}$$
$$= €\ value\ of\ total\ kgCO_2e\ saved\ [Case]_{ij} - Private\ Net\ Fuel\ Cost_{ij}$$

Equation (13)

$$\frac{total\ kgCO_2e\ saved_{(cruise)}}{passenger} = 0.08 \times (Route\ Distance - 280 - 281)$$

DOI: 10.14324/111.444.2755-0877.1856

Equation (14)

$$kgCO_2e\ saved\ (per\ route) = Passengers \times (43.15 + 4.87 + 0.08 \times (Distance - 280 - 281))$$

Equation (15)

$$Marginal\ Net\ Environmental\ Benefit_{ij}[Case] = External\ Carbon\ Cost \times Total\ kgCO_2e\ saved_{ij} \times CDF \times \eta \times \mu$$

where External Carbon Cost takes value €0.1034/kg in the high case, €0.0758/kg in the central case and €0.0285/kg in the low case.

Equation (16)

$$\begin{aligned} &Private\ Net\ Fuel\ Cost_{ij}[TaxQ] \\ &= \left(\frac{H_2\ €/Kg\ Airport\ i + H_2\ €/Kg\ Airport\ j}{2} \times \frac{GED_{Kerosene}(43\ MJ/kg)}{GED_{Hydrogen}(120\ MJ/kg)} - Kerosene\ Cost\ €/kg\right) \\ &\times Fuel\ Intensity \frac{kg}{min} \times Piecewise\ Distance\ km \times Speed^{-1}{}_{ij} \frac{min}{km} \\ &\times CDF \times Route's\ Annual\ Flight\ Count_{ij} \times \mu \times \tau \end{aligned}$$

where $\mathrm{CDF} = 1.09, \mu = 0.58, \tau = 1.49$ *and:*

$$\begin{aligned} &Kerosene\ Cost\ €/kg \\ &= 0.83595 \times 0.9361\ €/USD \times 1.0428^{27} + Which[TaxQ = 0,0, TaxQ = 1,0.55 \times 0.8kg/l] \end{aligned}$$

$$\begin{aligned} &Speed^{-1}{}_{ij} \frac{min}{km} \\ &= \big(110.80 \times 280.7 \times 16.24^{-1} + 45.98 \times (Distance - 280.7 \\ &\qquad - 280.9) \times 16.23^{-1} + 10.54 \times 280.9 \times 16.27^{-1}\big)_{ij} \end{aligned}$$

Appendix 2: Figures

Figure (1)

Emission	Emission Index (kg/kg kerosene)	GWP_{100}
CO_2	3.2	1.0
NO_x	0.0	25.0
Water vapour	1.2	0.1
Soot	3×10^{-5}	1,166.0
SO_2	1.2×10^{-3}	-226.0
Contrails (CO_2 basis)	-	0.6

DOI: 10.14324/111.444.2755-0877.1856

Figure 1: Assumptions for Kerosene Aircraft Emissions

Figure (2)

Emission	Kerosene	H_2 fuel cell	H_2 turbine
CO_2	100%	0%	0%
NO_x	100%	0%	35%
Water vapour	100%	250%	250%
Soot	100%	0%	0%
SO_2	100%	0%	0%
Contrails	100%	30%	60%

Figure 2: Hydrogen Aircraft Emissions Assumptions

Figure (3)

2050 External Cost of CO_2 (per tonne)

	Case (Discount Rate)		
Year Currency	Low (5%)	Central (3%)	High (2.5%)
2020 USD	32.0	85.0	116.0
2020 EUR	28.5	75.8	103.4

Figure 3: External Cost of CO_2

Figure (4)

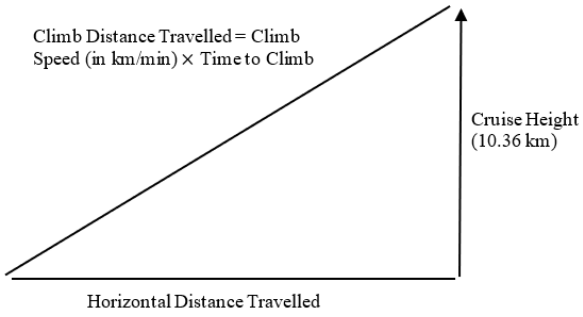

Figure 4: Visual Representation for Calculating Horizontal Distance Travelled (for climb)

DOI: 10.14324/111.444.2755-0877.1856

Figure (5)

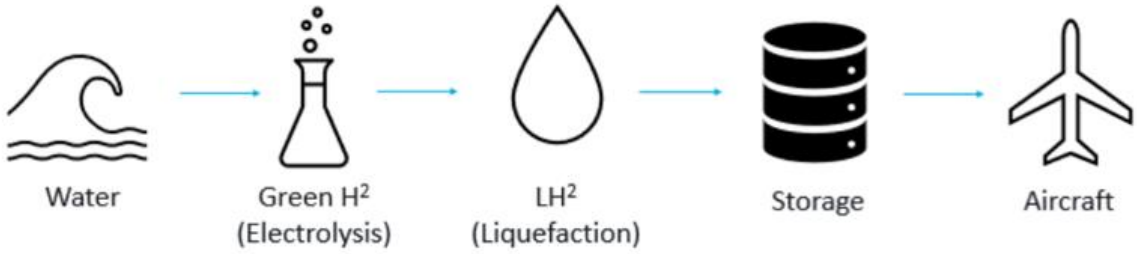

Figure 5: Hydrogen Value Chain

Figure (6)

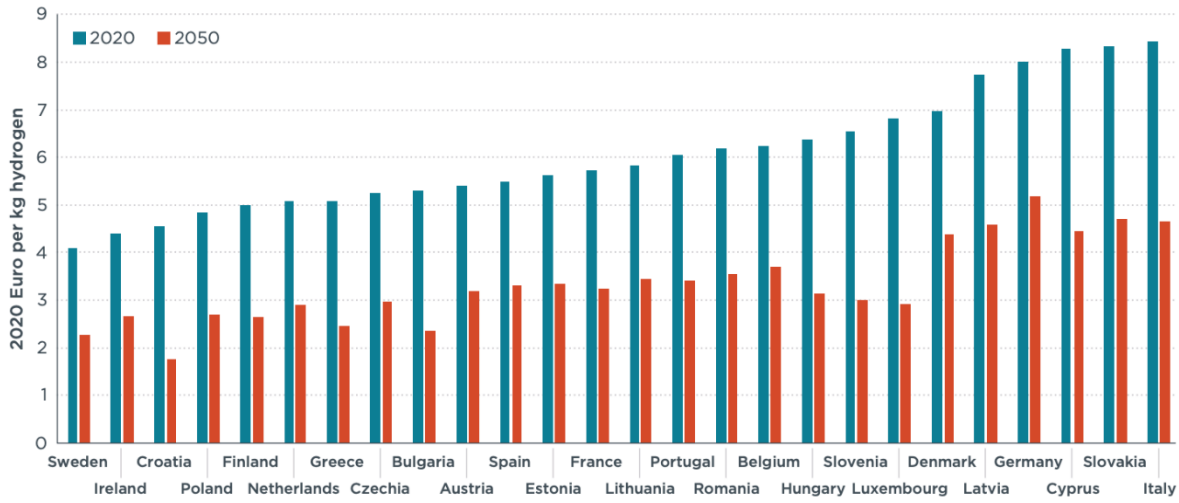

Figure 6: Hydrogen Production Costs per kg by Country (Zhou and Searle, 2020)

Figure (7)

Gearing Ratio (debt to equity)	60:40
Loan Interest Rate (Rd)	4%
Cost of Equity (Re)	16%
Corporate tax rate (t)	20.8%

Figure 7: WACC Assumptions

DOI: 10.14324/111.444.2755-0877.1856

Figure (8a)

Emission	Emission Index (kg/kg kerosene)	GWP_{100}	Emission (kg CO_2e/kg kerosene)
CO_2	3.2	1.0	3.2
NO_x	0.0	25.0	0.38
Water vapour	1.2	0.1	0.074
Soot	3×10^{-5}	1,166.0	0.035
SO_2	1.2×10^{-3}	-226.0	-0.27
Contrails (CO_2 basis)	-	0.6	2.0
Total CO_2 e			**5.4**

Figure 8a: Kerosene Aircraft Emissions

Figure (8b)

Emission	Emission (kg CO_2e/ kg kerosene)	Kg CO_2e for 0.36kg H_2 fuel cell / kg kerosene	Kg CO_2e for 0.36kg H_2 turbine / kg kerosene	Emission (kg CO_2e/ 0.36kg H_2 fuel cell)	Emission (kg CO_2e/ 0.36kg H_2 turbine)
CO_2	3.2	0	0	0	0
NO_x	0.38	0	0.35	0	0.13
Water vapour	0.074	2.5	2.5	0.18	0.18
Soot	0.035	0	0	0	0
SO_2	-0.271	0	0	0	0
Contrails	2.0	0.3	0.6	0.6	1.2
Total CO_2 e	**5.4**			**0.78**	**1.51**

Figure 8b: Hydrogen Aircraft Emissions

DOI: 10.14324/111.444.2755-0877.1856

Figure (9)

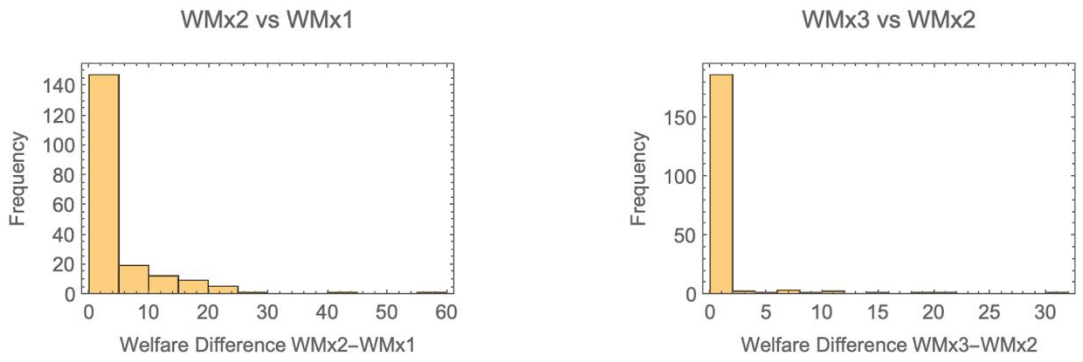

Figure 9: WMx algorithm comparison with successive orders

Figure (10)

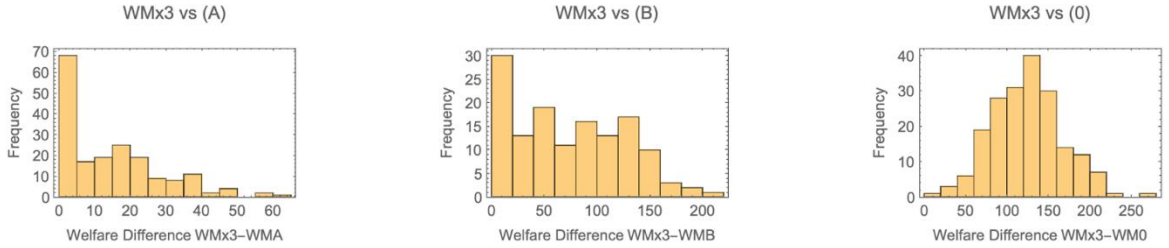

Figure 10: WMx3 algorithm comparison with (A), (B), (0) models

Figure (11)

	ρ=2.5%	ρ=3.0%	ρ=5.0%
Net Total Welfare Gain w/o kerosene Tax (€m)	3577.07	2786.24	1469.34
N# Airports Decarbonised w/o kerosene Tax	95	94	87
tCO2e Emissions Saved w/o kerosene Tax	370 023	367 437	348 867
% Emissions Saved w/o kerosene Tax	72.08%	71.58%	67.96%

	ρ=2.5%	ρ=3.0%	ρ=5.0%
Net Total Welfare Gain with €0.55/l Tax (€m)	6764.53	5913.72	4492.06
N# Airports Decarbonised with €0.55/l Tax	111	110	101
tCO2e Emissions Saved with €0.55/l Tax	399 872	398 211	381 856
% Emissions Saved with €0.55/l Tax	77.9%	77.57%	74.39%

Figure 11: Key variables for each of the 3 carbon cost scenarios, with and without €0.55/l tax

DOI: 10.14324/111.444.2755-0877.1856

Figure (12)

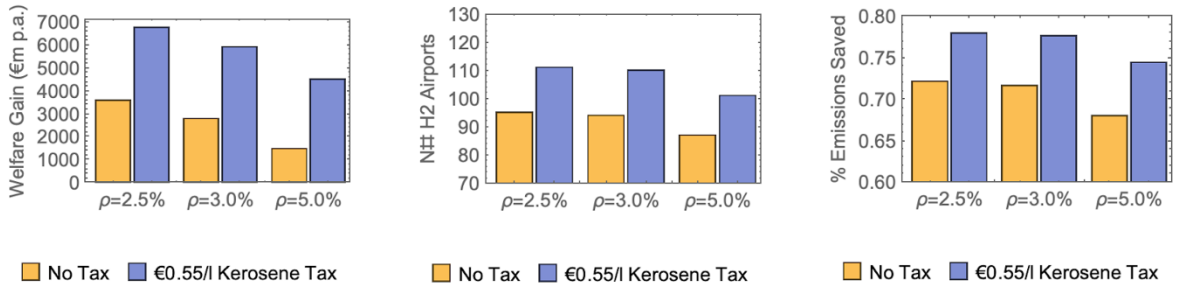

Figure 12: Key variables bar chart visualisation (note the plot range)

Figure (13)

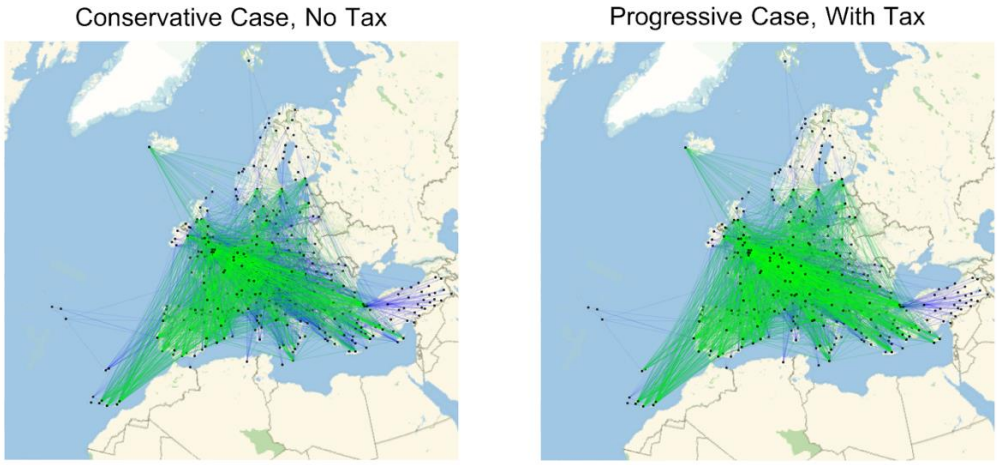

Figure 13: Decarbonised airport sub-network (green) overlaying main airports in EU+ (blue)

DOI: 10.14324/111.444.2755-0877.1856

Figure (14)

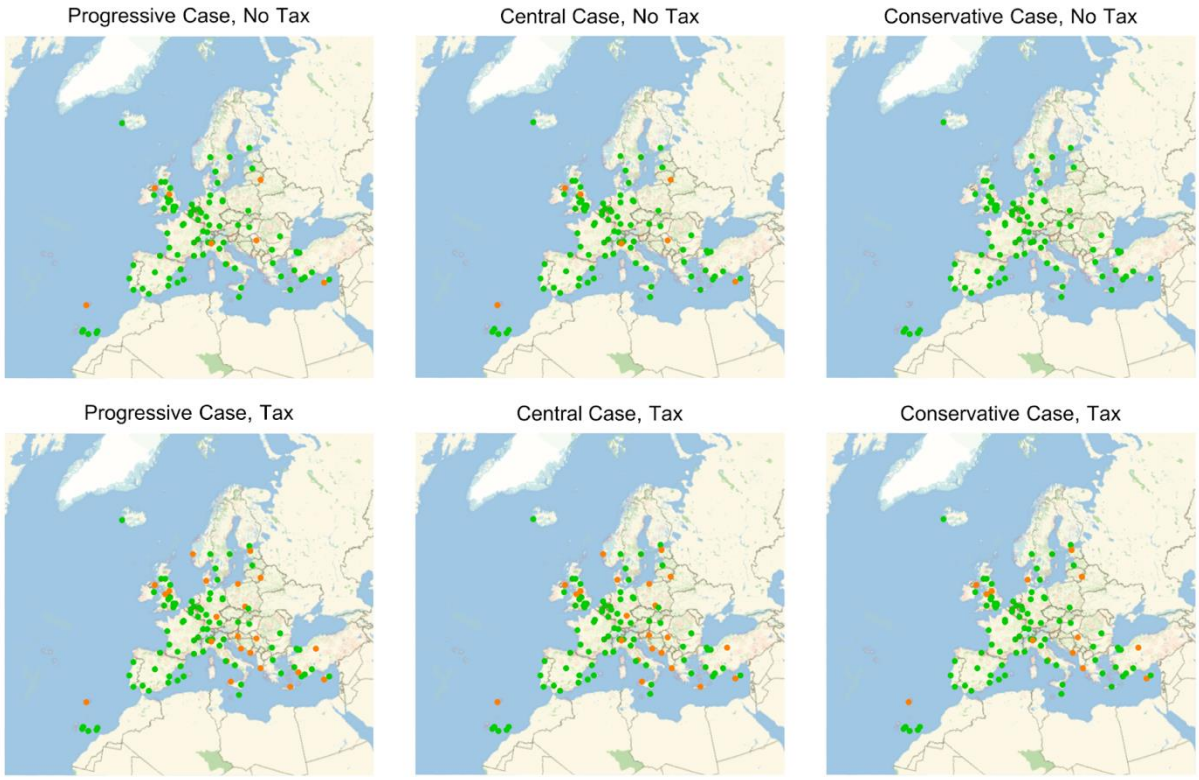

Figure 14: Decarbonised airport sub-network (green) and additional nodes decarbonised (orange) on top of 'Conservative Case, No Tax', with the conservative case having the highest discount rate

Figure (15)

	ρ=2.5%	ρ=3.0%	ρ=5.0%
Avg Passenger Degree as % of Original Network (no tax)	237.9%	239.1%	246.1%
Avg H2 Cost as % of Original Network (no tax)	104.7%	104.4%	104%
Global Clustering as % of Original Network (no tax)	208.94%	208.97%	209.15%
Avg Flight Distance as % of Original Network (no tax)	89.72%	90.05%	88.15%

	ρ=2.5%	ρ=3.0%	ρ=5.0%
Avg Passenger Degree as % of Original Network (w/ tax)	222.9%	223.8%	232.2%
Avg H2 Cost as % of Original Network (w/ tax)	102.6%	102.6%	103.9%
Global Clustering as % of Original Network (w/ tax)	208.62%	208.64%	208.81%
Avg Flight Distance as % of Original Network (w/ tax)	89.96%	89.53%	90.41%

Figure 15: Network Analytics comparison between decarbonised sub-networks and original

DOI: 10.14324/111.444.2755-0877.1856

Figure (16)

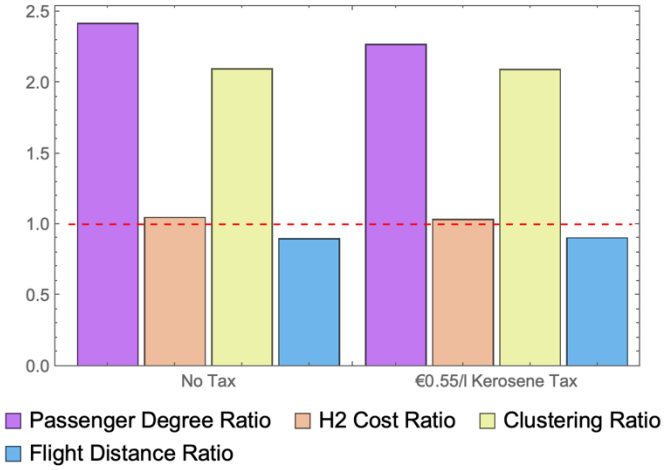

Figure 16: Network Analytics bar chart visualisation (mean across scenarios)

Appendix 3: Derivations of Select Equations

Derivation of equation (1)

$$\frac{kgCO_2e\ saved}{km \times \#\ seats\ occupied} = \frac{fuel\ (kg)}{time\ (min)} \times \frac{1}{speed\ (\%\ Mach)} \times \frac{Mach}{km/min} \times \frac{1}{\#\ seats\ available} \times \frac{\#\ seats\ available}{\#\ seats\ occupied} \times \frac{kgCO_2e\ saved\ (fuel\ cells)}{fuel\ (kg)}$$

where $\frac{\#\ seats\ available}{\#\ seats\ occupied} = \frac{1}{Load\ Factor}$, $\frac{Mach}{km/min} = 20.58$

We multiply fuel (kg)/min by 1 over the aircraft's average cruise speed (given as a fraction of Mach) and then by 20.58, the conversion factor of Mach to km/min. This is divided by the number of seats available on average in the aircraft, which is then multiplied by 1/load factor to account for the number of seats actually occupied. Finally, we multiply this by $kgCO_2e$ saved/kg fuel, which is 4.59 for fuel cells, to yield $kgCO_2e$ saved per pkm.

Derivation of equation (4)

$$\frac{Total\ kg\ CO_2e\ saved}{\#\ seats\ occupied} = \frac{fuel\ (kg)}{time\ (min)} \times \frac{1}{\#\ seats\ available} \times \frac{\#\ seats\ available}{\#\ seats\ occupied} \times \frac{kg\ CO_2e\ saved}{fuel\ (kg)} \times t$$

where t denotes total travel time.

We multiply it by 1/total seats available to estimate fuel consumption/available seat. This is multiplied by 1/load factor to get fuel consumption / occupied seat and is then multiplied by total time travelled for climb/descent (which are standardised) and multiplied by $kgCO_2e$ saved/kg fuel (which for climb is 3.86, for descent is 4.59).

DOI: 10.14324/111.444.2755-0877.1856

Appendix 4: Relationship between Fuel Consumption and Flight Level

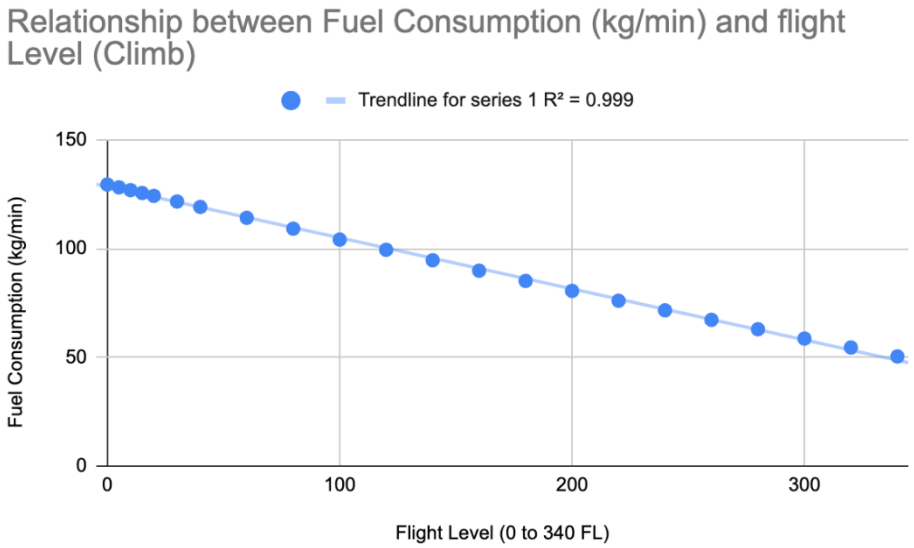

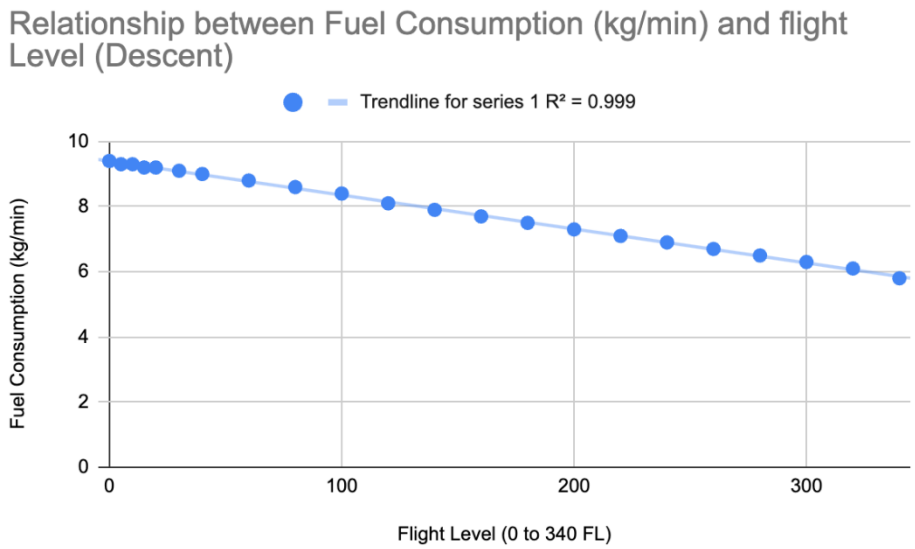

Above are the graphs demonstrating that the relationship between fuel consumption and flight level is highly linear (for the Airbus A320-200 model, for both climb and descent)

DOI: 10.14324/111.444.2755-0877.1856

Appendix 5: Tables for Weighted Averaging

Estimation of emissions saved during cruise

The table uses key figures from the BADA data set and GGR data sets, relevant for modelling cruise $\frac{kgCO_2e\ saved}{pkm}$. The right-most column is the resultant $kgCO_2$/pkm per aircraft model.

Model	Proportion Passenger km	fuel (kg) / time (min)	Seat Capacity	Load Factor	Cruise Speed (Mach)	$\frac{kgCO_2e\ saved}{pkm}$
AIRBUS A320neo	11%	38.1	183	86%	0.78	0.07
AIRBUS A321neo	8%	47.4	224	86%	0.78	0.07
AIRBUS A319	4%	40.0	149	86%	0.79	0.09
AIRBUS A320-100/200	17%	37.0	181	83%	0.78	0.07
AIRBUS A321	3%	49.3	223	85%	0.79	0.07
AIRBUS A330-300	1%	89.3	288	67%	0.81	0.13
BOEING 737 MAX 8	5%	37.0	194	90%	0.79	0.06
BOEING 737-800	44%	47.9	189	90%	0.79	0.08
BOEING 757-200	1%	48.9	220	94%	0.8	0.07
BOEING 767-300ER/F	1%	73.6	305	81%	0.8	0.08
BOEING 777-300ER	1%	117.2	344	79%	0.84	0.11

DOI: 10.14324/111.444.2755-0877.1856

BOEING 787-800 DREAMLINER	1%	69.8	244	85%	0.85	0.09
BOEING 787-900 DREAMLINER	1%	78.8	312	81%	0.85	0.08
Weighted average						**0.08**

Estimation of the weighted average of the horizontal distance of climb and descent

Model	Proportion Passenger km	Climb Speed (Mach)	Descent Speed (Mach)	Horizontal Distance (Climb)	Horizontal Distance (Descent)
AIRBUS A320neo	11%	0.78	0.78	277	277
AIRBUS A321neo	8%	0.78	0.78	277	277
AIRBUS A319	4%	0.78	0.78	277	277
AIRBUS A320-100/200	17%	0.78	0.78	277	277
AIRBUS A321	3%	0.78	0.78	277	277
AIRBUS A330-300	1%	0.8	0.8	284	284
BOEING 737 MAX 8	5%	0.78	0.78	277	277
BOEING 737-800	44%	0.8	0.8	284	284
BOEING 757-200	1%	0.78	0.78	277	277
BOEING 767-300ER/F	1%	0.72	0.72	256	256
BOEING 777-300ER	1%	0.83	0.84	295	299
BOEING 787-800 DREAMLINER	1%	0.79	0.84	280	299
BOEING 787-900 DREAMLINER	1%	0.79	0.84	280	299
Weighted average				**280**	**281**

DOI: 10.14324/111.444.2755-0877.1856

Estimation of the emission savings for climb and descent

Model	Proportion Passenger km	Climb Fuel kg/min (0 FL)	Climb Fuel kg/min (340 FL)	Descent Fuel kg/min (0 FL)	Descent Fuel kg/min (340 FL)	Total $kgCO_2$/ passenger Climb	Total $kgCO_2$/ passenger Descent
AIRBUS A320neo	11%	122.0	57.2	10.6	8.0	37.9	4.7
AIRBUS A321neo	8%	151.7	71.2	13.1	10.0	38.5	4.7
AIRBUS A319	4%	128.1	60.1	11.1	8.4	48.9	6.0
AIRBUS A320-100/200	17%	129.4	50.4	9.4	5.8	39.8	4.0
AIRBUS A321	3%	157.8	74.0	13.7	10.4	40.7	5.0
AIRBUS A330-300	1%	401.5	144.9	22.2	15.3	94.2	7.7
BOEING 737 MAX 8	5%	118.5	55.6	10.3	7.8	33.2	4.1
BOEING 737-800	44%	149.5	82.0	11.9	9.5	45.3	5.0
BOEING 757-200	1%	177.5	81.4	18.4	16.2	41.7	6.6
BOEING 767-300ER/F	1%	235.7	110.6	20.4	15.5	46.6	5.8
BOEING 777-300ER	1%	375.1	176.0	32.5	24.6	67.5	8.3
BOEING 787-800 DREAMLINER	1%	223.4	104.8	19.3	14.7	52.7	6.5
BOEING 787-900 DREAMLINER	1%	252.3	118.4	21.8	16.6	48.8	6.0
Weighted average						**43.15**	**4.87**

DOI: 10.14324/111.444.2755-0877.1856

Appendix 6: Mathematica Code

Notebook file available on request to authors or UJE

Optimisation Algorithms

```
(*Note: Each algorithm uses input matrix with elements {MBR,i,j} where i,
j are its row and column numbers respectively. This is done to
 track node index. Note also that all matrices are symmetrical*)
```

WMx1

In[1]:=
```
WMx1[WGraphG_, CostC_] :=
 Module[{ActiveSG = WGraphG}, While[Length[ActiveSG[[All, All, 1]]] > 1,
   DegreeList = ActiveSG[[All, All, 1]].Table[1, {Length[ActiveSG[[All, All, 1]]]}];
   PrunePos = Position[DegreeList, Min[DegreeList]][[1, 1]];
   If[DegreeList[[PrunePos]] < CostC,
    ActiveSG = Drop[ActiveSG, {PrunePos}, {PrunePos}], Break[]]];
  If[Total[Total[ActiveSG[[All, All, 1]]]] / 2 - Length[ActiveSG[[All, All, 1]]] *
      CostC < 0, NewGraphGWMx1 = 0, NewGraphGWMx1 = ActiveSG];
  NewGraphGWMx1]
```

WMx2

In[2]:=
```
WMx2[WGraphG_, CostC_] := Module[
  {ActiveSG = WGraphG, PruneOrder = 1}, While[Length[ActiveSG[[All, All, 1]]] > 1,
   Which[PruneOrder == 1, While[Length[ActiveSG[[All, All, 1]]] > 1, DegreeList =
      ActiveSG[[All, All, 1]].Table[1, {Length[ActiveSG[[All, All, 1]]]}];
     PrunePos = Position[DegreeList, Min[DegreeList]][[1, 1]];
     If[DegreeList[[PrunePos]] < CostC,
      ActiveSG = Drop[ActiveSG, {PrunePos}, {PrunePos}], PruneOrder++;
      Break[]]], PruneOrder == 2, While[Length[ActiveSG[[All, All, 1]]] > 1,
     DegreeList = ActiveSG[[All, All, 1]].
       Table[1, {Length[ActiveSG[[All, All, 1]]]}];
     DegreeMat = Outer[Plus, DegreeList, DegreeList] - ActiveSG[[All, All, 1]];
     DegreeMat = Table[If[Length[Union[{i1, j1}]] < 2, Infinity,
        DegreeMat[[i1, j1]]], {i1, Length[DegreeMat]}, {j1, Length[DegreeMat]}];
     PrunePos = Position[DegreeMat, Min[DegreeMat]][[1]];
     If[DegreeMat[[PrunePos[[1]], PrunePos[[2]]]] < 2 * CostC,
      ActiveSG = Drop[Drop[ActiveSG, {Max[PrunePos]}, {Max[PrunePos]}],
        {Min[PrunePos]}, {Min[PrunePos]}];
      PruneOrder = 1;
      Break[], PruneOrder = 0;
      Break[]]], PruneOrder == 0, Break[]];];
  If[Total[Total[ActiveSG[[All, All, 1]]]] / 2 - Length[ActiveSG[[All, All, 1]]] *
      CostC < 0, NewGraphGWMx2 = 0, NewGraphGWMx2 = ActiveSG];
  NewGraphGWMx2]
```


DOI: 10.14324/111.444.2755-0877.1856

WMx3

In[3]:=
```
WMx3[WGraphG_, CostC_] := Module[
  {ActiveSG = WGraphG, PruneOrder = 1}, While[Length[ActiveSG[[All, All, 1]]] > 1,
   Which[PruneOrder == 1, While[Length[ActiveSG[[All, All, 1]]] > 1, DegreeList =
       ActiveSG[[All, All, 1]].Table[1, {Length[ActiveSG[[All, All, 1]]]}];
     PrunePos = Position[DegreeList, Min[DegreeList]][[1, 1]];
     If[DegreeList[[PrunePos]] < CostC,
      ActiveSG = Drop[ActiveSG, {PrunePos}, {PrunePos}], PruneOrder++;
      Break[]]], PruneOrder == 2, While[Length[ActiveSG[[All, All, 1]]] > 1,
     DegreeList = ActiveSG[[All, All, 1]].
       Table[1, {Length[ActiveSG[[All, All, 1]]]}];
     DegreeMat = Outer[Plus, DegreeList, DegreeList] - ActiveSG[[All, All, 1]];
     DegreeMat = Table[If[Length[Union[{i1, j1}]] < 2, Infinity,
        DegreeMat[[i1, j1]]], {i1, Length[DegreeMat]}, {j1, Length[DegreeMat]}];
     PrunePos = Position[DegreeMat, Min[DegreeMat]][[1]];
     If[DegreeMat[[PrunePos[[1]], PrunePos[[2]]]] < 2 * CostC,
      ActiveSG = Drop[Drop[ActiveSG, {Max[PrunePos]}, {Max[PrunePos]}],
        {Min[PrunePos]}, {Min[PrunePos]}];
      PruneOrder = 1;
      Break[], PruneOrder++;
      Break[]]], PruneOrder == 3,
    While[Length[ActiveSG[[All, All, 1]]] > 1, DegreeList =
      ActiveSG[[All, All, 1]].Table[1, {Length[ActiveSG[[All, All, 1]]]}];
     DegreeMat = Table[DegreeList[[i]] + DegreeList[[j]] -
        ActiveSG[[All, All, 1]][[j, i]] + DegreeList[[k]] - ActiveSG[[All, All, 1]][[k, i]] -
        ActiveSG[[All, All, 1]][[k, j]], {i, Length[ActiveSG[[All, All, 1]]]},
       {j, Length[ActiveSG[[All, All, 1]]]}, {k, Length[ActiveSG[[All, All, 1]]]}];
     DegreeMat = Table[If[Length[Union[{i1, j1, k1}]] < 3, Infinity,
        DegreeMat[[i1, j1, k1]]], {i1, Length[DegreeMat]},
       {j1, Length[DegreeMat]}, {k1, Length[DegreeMat]}];
     PrunePos = Position[DegreeMat, Min[DegreeMat]][[1]];
     If[DegreeMat[[PrunePos[[1]], PrunePos[[2]], PrunePos[[3]]]] < 3 * CostC,
      ActiveSG = Drop[Drop[Drop[ActiveSG, {Max[PrunePos]}, {Max[PrunePos]}],
         {Sort[PrunePos, Less][[-2]]}, {Sort[PrunePos, Less][[-2]]}],
        {Min[PrunePos]}, {Min[PrunePos]}];
      PruneOrder = 1;
      Break[], PruneOrder = 0;
      Break[]]], PruneOrder == 0, Break[]];];
  If[Total[Total[ActiveSG[[All, All, 1]]]] / 2 - Length[ActiveSG[[All, All, 1]]] *
      CostC < 0, NewGraphGWMx3 = 0, NewGraphGWMx3 = ActiveSG];
  NewGraphGWMx3]
```


DOI: 10.14324/111.444.2755-0877.1856

(A) Weighted Degree Centrality Ranking

In[4]:=
```
WMA[WGraphG_, CostC_] := Module[{ActiveSG = WGraphG},
  DegreeList = ActiveSG[[All, All, 1]].Table[1, {Length[ActiveSG[[All, All, 1]]}];
  PrunePos = Position[DegreeList, x_ /; x < CostC] // Flatten;
  For[i = 1, i ≤ Length[PrunePos], i++,
   ActiveSG = Drop[ActiveSG, {PrunePos[[i]] - i + 1}, {PrunePos[[i]] - i + 1}]];
  If[Total[Total[ActiveSG[[All, All, 1]]]] / 2 - Length[ActiveSG[[All, All, 1]]] *
      CostC < 0, NewGraphGA = 0, NewGraphGA = ActiveSG];
  NewGraphGA]
```

(B) Weighted Eigenvector Centrality Ranking

In[5]:=
```
WMB[WGraphG_, CostC_] := Module[
  {ActiveSG = WGraphG, WelfareList = {}}, While[Length[ActiveSG[[All, All, 1]]] > 1,
   WelfareList = Append[WelfareList, (Total[Total[ActiveSG[[All, All, 1]]]] / 2 -
       Length[ActiveSG[[All, All, 1]]] * CostC)];
   PruneMinEVCPos = Position[Eigenvectors[N[ActiveSG[[All, All, 1]], 5]][[1]],
      Min[Eigenvectors[N[ActiveSG[[All, All, 1]], 5]][[1]]]][[1, 1]];
   ActiveSG = Drop[ActiveSG, {PruneMinEVCPos}, {PruneMinEVCPos}]];
  AppendTo[WelfareList, 0];
  OptimalTime = Position[WelfareList, Max[WelfareList]][[1, 1]];
  ActiveSG = WGraphG;
  If[OptimalTime == Length[WGraphG[[All, All, 1]]], NewGraphGB = 0, While[
    OptimalTime > 1, PruneMinEVCPos = Position[Eigenvectors[N[ActiveSG[[All, All,
           1]], 5]][[1]], Min[Eigenvectors[N[ActiveSG[[All, All, 1]], 5]][[1]]]][[1, 1]];
    ActiveSG = Drop[ActiveSG, {PruneMinEVCPos}, {PruneMinEVCPos}];
    OptimalTime = OptimalTime - 1;];
   If[Total[Total[ActiveSG[[All, All, 1]]]] / 2 - Length[ActiveSG[[All, All, 1]]] *
       CostC < 0, NewGraphGB = 0, NewGraphGB = ActiveSG];];
  NewGraphGB]
```

Welfare Function (equivalent to (0) Case)

In[6]:=
```
Welfare[AdjMat_, CostC_] := Total[Total[AdjMat]] / 2 - Length[AdjMat] * CostC
```


DOI: 10.14324/111.444.2755-0877.1856

Comparison of WMx1, WMx2, WMx3, (A), (B), and (0):

In[7]:=
```
(*Sample of Toy Graphs*)
NC = 40;
EC = 80;
CostC = 1 * NC;
SSize = 200;

SampleGraphs = Table[Module[{GraphG = AdjacencyMatrix[RandomGraph[{NC, EC}]],
      UniformWeighting = Table[RandomReal[{0, NC}], {i, 1, NC}, {j, 1, NC}]},
    SymUniWeighting = ((UniformWeighting + Transpose[UniformWeighting]) / 2);
    WGraphG = Table[{SymUniWeighting[[i, j]] * GraphG[[i, j]], i, j},
      {i, 1, NC}, {j, 1, NC}]], {SSize}];
```

In[ ]:=
```
(*Comparison of WMx Algorithms*)
GraphicsGrid[
 {{Histogram[Table[Welfare[WMx2[SampleGraphs[[i]], CostC]][[All, All, 1]], CostC] -
      Welfare[WMx1[SampleGraphs[[i]], CostC]][[All, All, 1]], CostC], {i, 1, SSize}],
    10, Frame → True, PlotLabel → "WMx2 vs WMx1", FrameLabel →
     {"Welfare Difference WMx2-WMx1", "Frequency"}, PlotRange → All],
   Histogram[Table[Welfare[WMx3[SampleGraphs[[i]], CostC]][[All, All, 1]], CostC] -
      Welfare[WMx2[SampleGraphs[[i]], CostC]][[All, All, 1]], CostC], {i, 1, SSize}],
    10, Frame → True, PlotLabel → "WMx3 vs WMx2", FrameLabel →
     {"Welfare Difference WMx3-WMx2", "Frequency"}, PlotRange → All]}}]
```

Out[ ]=

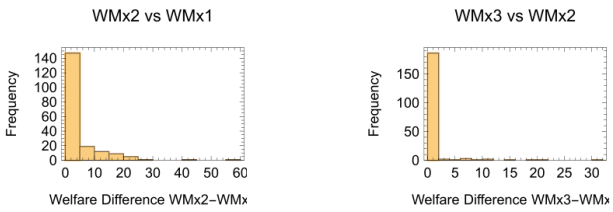


```
(*Comparison of WMx3 vs (A), (B), and (0)*)
```


DOI: 10.14324/111.444.2755-0877.1856

```
In[•]:= GraphicsGrid[
 {{Histogram[Table[Welfare[WMx3[SampleGraphs[[i]], CostC]][All, All, 1]], CostC] -
      Welfare[WMA[SampleGraphs[[i]], CostC]][All, All, 1]], CostC], {i, 1, SSize}],
    10, Frame → True, PlotLabel → "WMx3 vs (A)",
    FrameLabel → {"Welfare Difference WMx3-WMA", "Frequency"}, PlotRange → All],
   Histogram[Table[Welfare[WMx3[SampleGraphs[[i]], CostC]][All, All, 1]], CostC] -
      Welfare[WMB[SampleGraphs[[i]], CostC]][All, All, 1]], CostC], {i, 1, SSize}],
    10, Frame → True, PlotLabel → "WMx3 vs (B)",
    FrameLabel → {"Welfare Difference WMx3-WMB", "Frequency"}, PlotRange → All],
   Histogram[Table[Welfare[WMx3[SampleGraphs[[i]], CostC]][All, All, 1]], CostC] -
      Welfare[SampleGraphs[[i]][All, All, 1]], CostC], {i, 1, SSize}],
    10, Frame → True, PlotLabel → "WMx3 vs (0)", FrameLabel →
     {"Welfare Difference WMx3-WM0", "Frequency"}, PlotRange → All]}}]
```

Out[•]=

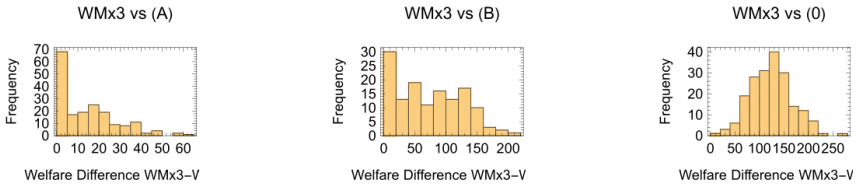


```
(*Network Density Mismatch*)
```

```
In[12]:= ToyDensity = 80 / (0.5 * 40 * (40 - 1))
         RealDensity = 9252 / (0.5 * 345 * (345 - 1))
```

Out[12]=

```
0.102564
```

Out[13]=

```
0.155915
```

Network Processing

```
In[14]:= (*Relevant Imports*)
         AirportCoordinates =
           Import["/Users/hexagon/Downloads/Files Prev/FINAL airports
                and coordinates.xlsx"][[1]];
         PAXlist = Import["/Users/hexagon/Downloads/Files Prev/Routes FINAL.xlsx"][[1]];
         Flightlist =
           Import["/Users/hexagon/Downloads/Files Prev/FINAL flight count.xlsx"][[1]];
         HydroCost50 = Import["/Users/hexagon/Downloads/Files Prev/H2 costs.xlsx"][[1]];
```

```
In[18]:= (*Distance Matrix*)
         DstMat = Table[
            UnitConvert[GeoDistance[{AirportCoordinates[[j, 2]], AirportCoordinates[[j, 3]]},
              {AirportCoordinates[[k, 2]], AirportCoordinates[[k, 3]]}],
             "Kilometers"], {j, 345}, {k, 345}];
```


DOI: 10.14324/111.444.2755-0877.1856

In[19]:=
```
(*Airport List And Passenger Count Matrix Cleaning*)
Arptlist = Table[AirportCoordinates[[j, 1]], {j, 345}];
EmptyMat = Table[0, 345, 345];
OrdPAXlist = Catch[
    For[i = 1;
     OrdPaxlist = EmptyMat, i ≤ 4626, i++,
     OrdPaxlist = ReplaceAt[OrdPaxlist, 0 → PAXlist[[i, 3]],
       {Flatten[Position[Arptlist, PAXlist[[i, 1]]]][[1]],
        Flatten[Position[Arptlist, PAXlist[[i, 2]]]][[1]]}];
     If[i == 4626, Throw[OrdPaxlist]]]];
PAXMat = 1 / 2 (OrdPAXlist + Transpose[OrdPAXlist]) /. 0 → ∞;
```

In[23]:=
```
(*Flight Count Matrix Cleaning*)
OrdFlightlist = Catch[
    For[i = 1;
     OrdFlightlist = EmptyMat, i ≤ Length[Flightlist], i++,
     OrdFlightlist = ReplaceAt[OrdFlightlist, 0 → Flightlist[[i, 3]],
       {Flatten[Position[Arptlist, Flightlist[[i, 1]]]][[1]],
        Flatten[Position[Arptlist, Flightlist[[i, 2]]]][[1]]}];
     If[i == Length[Flightlist], Throw[OrdFlightlist]]]];
FlightMat = 1 / 2 (OrdFlightlist + Transpose[OrdFlightlist]) /. 0 → ∞;
```

In[25]:=
```
(*Cleaning Origins and Destinations*)
Origins = Table[Flightlist[[j, 1]], {j, Length[Flightlist]}];
Destinations = Table[Flightlist[[j, 2]], {j, Length[Flightlist]}];
Emptylist = Table[0, Length[Arptlist]];
Countries = Catch[For[i = 1;
     ListA = Emptylist, i ≤ Length[Arptlist], i++,
     ListA = ReplaceAt[ListA, 0 → If[NumberQ[Position[Origins, Arptlist[[i]]][[1, 1]]],
         Flightlist[[Position[Origins, Arptlist[[i]]][[1, 1]], 4]],
         Flightlist[[Position[Destinations, Arptlist[[i]]][[1, 1]], 4]], {i}];
     If[i == Length[Arptlist], Throw[ListA]]]];
```

In[29]:=
```
(*Hydrogen Costs - average of origin and destination airport taken*)
CtryH2Cost =
  Table[HydroCost50[[Position[HydroCost50, Countries[[j]]][[1, 1]], 2]], {j, 345}];
H2CostMat =
  0.5 (CtryH2Cost⊗Table[1, 345] + Transpose[CtryH2Cost⊗Table[1, 345]] /. {} → 0);

(*Constructing Multi-variable Matrix to encapsulate all heterogenous data*)
FinalMat = Table[{DstMat[[j, k]], H2CostMat[[j, k]],
      If[PAXMat[[j, k]] == ∞ || FlightMat[[j, k]] == ∞, ∞, FlightMat[[j, k]]],
      If[PAXMat[[j, k]] == ∞ || FlightMat[[j, k]] == ∞, ∞, PAXMat[[j, k]]],
      Arptlist[[j]], Arptlist[[k]]}, {j, 345}, {k, 345}] /. {∞ → 0};
```


DOI: 10.14324/111.444.2755-0877.1856

In[32]:=
```
(*Defining Functions Required*)
kgCO2SavedPR[Passengers_, Distance_] :=
  Passengers * (43.15 + 4.87 + 0.08 * (Distance - 280 - 281));
MarginalNetEnviBenefit[Case_, Passengers_, Distance_] :=
 kgCO2SavedPR[Passengers, Distance] * 1.09 * 0.58 * 1.66 *
  Which[Case == "High", 0.1034, Case == "Medium", 0.0758, Case == "Low", 0.0285]
PrivateNetFuelCost[AvgH2Cost_, Distance_, FlightCount_, TaxQ_] :=
   (Max[(AvgH2Cost), 0] * 43/120 -
      ((0.83595 * 0.9361) * 1.0428448^27 + Which[TaxQ == 0, 0, TaxQ == 1, 0.55 * 0.8])) *
    (110.80 * 280.70 * 16.24^-1 + 45.98 * (Distance - 280.70 - 280.90) * 16.23^-1 +
      10.54 * 280.90 * 16.27^-1) * 1.09 * FlightCount * 0.58 * 1.49;
MBR[Passengers_, Distance_, FlightCount_, AvgH2Cost_, Case_, TaxQ_] :=
 MarginalNetEnviBenefit[Case, Passengers, Distance] -
  PrivateNetFuelCost[AvgH2Cost, Distance, FlightCount, TaxQ]
```

In[36]:=
```
(*Transforming Data in Final Mat to form MBR Network*)
MBRList = Table[Module[{VarList = FinalMat[[j, k]]}, {MBR[VarList[[4]],
      QuantityMagnitude[VarList[[1]]], VarList[[3]], VarList[[2]], case, taxq], j, k}],
   {taxq, {0, 1}}, {case, {"High", "Medium", "Low"}},
   {j, 1, Length[FinalMat]}, {k, 1, Length[FinalMat]}];
```

In[37]:=
```
(*Environmental Impact Comparison
 (Emissions saved as % of all EU commercial aviation emissions)*)
InitialTotalEnviImpact = Total[Total[
   Table[kgCO2SavedPR[FinalMat[[j, k]][[3]], QuantityMagnitude[FinalMat[[j, k]][[1]]]],
    {j, 1, Length[FinalMat]}, {k, 1, Length[FinalMat]}]]]
 (*For context: kgCO2e emitted in 2050 by EU commercial aviation*)
```

Out[37]=
$$5.13338 \times 10^8$$

In[38]:=
```
EnviImpact[SubGraphIndexList_] := Module[
  {subgraph = FinalMat[[SubGraphIndexList]][[All, SubGraphIndexList]]}, Total[Total[
    Table[kgCO2SavedPR[subgraph[[j, k]][[3]], QuantityMagnitude[subgraph[[j, k]][[1]]]],
     {j, 1, Length[subgraph]}, {k, 1, Length[subgraph]}]]]]


(*Modelling Scenarios -
 NOTE: can change to WMx1 for significantly faster runtimes;
 all WMx optimal sub-networks are identical in our case*)
```


DOI: 10.14324/111.444.2755-0877.1856

```
CostC = (2 * 15.9 + 33.37) * 1 000 000;
RnDCost = 1.11 * 1 000 000 000;
ResultsGrid = {, };
SaveList = Table[0, {2}, {3}];
For[taxq = 0, taxq ≤ 1, taxq++,
 ResultsGrid[[taxq + 1]] = Grid[{{"", "ρ=2.5%", "ρ=3.0%", "ρ=5.0%"}, Flatten[
     Append[{Which[taxq == 0, "Net Total Welfare Gain w/o kerosene Tax (€m)",
        taxq == 1, "Net Total Welfare Gain with €0.55/l Tax (€m)"]},
       Table[Round[(Welfare[WMx3[MBRList[[taxq + 1]][[CaseNum]], CostC][[All, All, 1]],
            CostC] - RnDCost) / 10^6, 0.001], {CaseNum, 1, 3}]]],
    Flatten[Append[{Which[taxq == 0, "N# Airports Decarbonised w/o kerosene Tax",
        taxq == 1, "N# Airports Decarbonised with €0.55/l Tax"]}, Table[Length[
        WMx3[MBRList[[taxq + 1]][[CaseNum]], CostC][[All, All, 1]], {CaseNum, 1, 3}]]],
    Flatten[Append[{Which[taxq == 0, "tCO2e Emissions Saved w/o kerosene Tax",
        taxq == 1, "tCO2e Emissions Saved with €0.55/l Tax"]},
       Table[Round[EnviImpact[WMx3[MBRList[[taxq + 1]][[CaseNum]], CostC][[
            All, All, 2]][[All, 1]], 10^3] / 10^3, {CaseNum, 1, 3}]]],
    Flatten[Append[{Which[taxq == 0, "% Emissions Saved w/o kerosene Tax",
        taxq == 1, "% Emissions Saved with €0.55/l Tax"]},
       Table[PercentForm[SaveList[[taxq + 1, CaseNum]] = EnviImpact[
            WMx3[MBRList[[taxq + 1]][[CaseNum]], CostC][[All, All, 2]][[All, 1]]] /
          InitialTotalEnviImpact], {CaseNum, 1, 3}]]], Frame → All,
   Background → {{Opacity[0.5, Gray]}, {Opacity[0.5, Gray]}}]]
```

In[49]:=
```
ResultsGrid[[1]]
ResultsGrid[[2]]
```

Out[49]=

	ρ=2.5%	ρ=3.0%	ρ=5.0%
Net Total Welfare Gain w/o kerosene Tax (€m)	3577.07	2786.24	1469.34
N# Airports Decarbonised w/o kerosene Tax	95	94	87
tCO2e Emissions Saved w/o kerosene Tax	370 023	367 437	348 867
% Emissions Saved w/o kerosene Tax	72.08%	71.58%	67.96%

Out[50]=

	ρ=2.5%	ρ=3.0%	ρ=5.0%
Net Total Welfare Gain with €0.55/l Tax (€m)	6764.53	5913.72	4492.06
N# Airports Decarbonised with €0.55/l Tax	111	110	101
tCO2e Emissions Saved with €0.55/l Tax	399 872	398 211	381 856
% Emissions Saved with €0.55/l Tax	77.9%	77.57%	74.39%

```
(*Barchart of Results*)
```


DOI: 10.14324/111.444.2755-0877.1856

In[51]:=
```
GraphicsGrid[
 {{BarChart[Transpose[{ResultsGrid[[1, 1, 2]][[2 ;;]], ResultsGrid[[2, 1, 2]][[2 ;;]]}],
    Frame → True, FrameLabel → {"", "Welfare Gain (€m p.a.)"},
    ChartLabels → {ResultsGrid[[1, 1, 1]][[2 ;;]], None},
    ChartLegends → Placed[{"No Tax", "€0.55/l Kerosene Tax"}, Bottom]],
   BarChart[Transpose[{ResultsGrid[[1, 1, 3]][[2 ;;]], ResultsGrid[[2, 1, 3]][[2 ;;]]}],
    Frame → True, FrameLabel → {"", "N# H2 Airports"},
    ChartLabels → {ResultsGrid[[1, 1, 1]][[2 ;;]], None},
    PlotRange → {70, 130}, PlotRangeClipping → True,
    ChartLegends → Placed[{"No Tax", "€0.55/l Kerosene Tax"}, Bottom]],
   BarChart[Transpose[SaveList], Frame → True, FrameLabel →
     {"", "% Emissions Saved"}, ChartLabels → {ResultsGrid[[1, 1, 1]][[2 ;;]], None},
    PlotRange → {0.6, 0.8}, PlotRangeClipping → True,
    ChartLegends → Placed[{"No Tax", "€0.55/l Kerosene Tax"}, Bottom]]}}]
```

Out[51]=

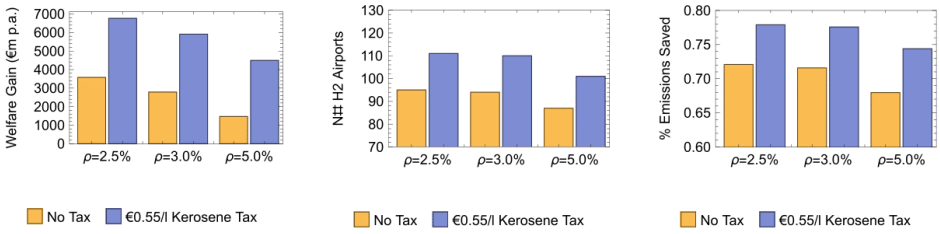


```
(*Kerosene % Real Price Annual Growth Rate*)
```

In[52]:=
```
((3.374 / 0.85)^(1/22) - 1) - ((124.27 / 78.97)^(1/21) - 1)
```

Out[52]=

```
0.0428448
```

Analysis of Results

In[62]:=
```
(*Network Tools - Borrowed from UCL ECON0114*)
VectorOfOnes[n_] := Table[1, n]
din[A_] := VectorOfOnes[Length[A]].A
Triangles[A_] := Diagonal[MatrixPower[A, 3]]
MA[k_] := Table[1, {j, 1, k}, {n, 1, k}] - IdentityMatrix[k]
TwoStep[A_] := Diagonal[A .MA[Length[A]].A]
WattsStrogatz[A_, j_] :=
 Module[{ws1 = Triangles[A][[j]], ws2 = TwoStep[A][[j]]}, If[ws2 == 0, 0, ws1/ws2]]
```

In[68]:=
```
(*Average Passenger Count Degree Centrality*)
AvgPaxCentralityRatio[SubGraphIndexList_] :=
 Module[{subgraph = FinalMat[[SubGraphIndexList]][[All, SubGraphIndexList]]},
   Mean[din[subgraph[[All, All, 3]]]] / Mean[din[FinalMat[[All, All, 3]]]]
```


DOI: 10.14324/111.444.2755-0877.1856

In[69]:=
```
(*Average H2 Cost*)
AvgH2CostRatio[SubGraphIndexList_] :=
 Module[{subgraph = FinalMat[[SubGraphIndexList]][[All, SubGraphIndexList]]},
   Mean[Diagonal[subgraph[[All, All, 2]]]] / Mean[Diagonal[FinalMat[[All, All, 2]]]]
```

In[70]:=
```
(*Unitized Network Global Clustering Coefficient Comparison*)
ClusteringRatio[SubGraphIndexList_] :=
 Module[{subgraph = FinalMat[[SubGraphIndexList]][[All, SubGraphIndexList]]},
  Mean[Table[N[WattsStrogatz[Unitize[subgraph[[All, All, 2]]], j], 5],
     {j, Length[subgraph]}]] /
   Mean[Table[N[WattsStrogatz[Unitize[FinalMat[[All, All, 3]]], j], 5],
     {j, Length[FinalMat]}]]]
```

In[71]:=
```
(*Average Distance Comparison*)
AvgDistanceRatio[SubGraphIndexList_] :=
 Module[{subgraph = FinalMat[[SubGraphIndexList]][[All, SubGraphIndexList]]},
   Mean[Mean[QuantityMagnitude[subgraph[[All, All, 1]]]]] /
  Mean[Mean[QuantityMagnitude[FinalMat[[All, All, 1]]]]]

(*Network Comparison Table*)
SaveList2 = Table[0, {4}, {2}, {3}];
AnalysisGrid = {, };
For[taxq = 0, taxq ≤ 1, taxq++,
 AnalysisGrid[[taxq + 1]] =
  Grid[{{"", "ρ=2.5%", "ρ=3.0%", "ρ=5.0%"}, Flatten[Append[{Which[taxq == 0,
        "Avg Passenger Degree as % of Original Network (no tax)", taxq == 1,
        "Avg Passenger Degree as % of Original Network (w/ tax)"]},
      Table[PercentForm[SaveList2[[1, taxq + 1, CaseNum]] = AvgPaxCentralityRatio[
          WMx3[MBRList[[taxq + 1]][[CaseNum]], CostC][[All, All, 2]][[All, 1]]],
       {CaseNum, 1, 3}]]], Flatten[Append[{Which[taxq == 0,
        "Avg H2 Cost as % of Original Network (no tax)", taxq == 1,
        "Avg H2 Cost as % of Original Network (w/ tax)"]},
      Table[PercentForm[SaveList2[[2, taxq + 1, CaseNum]] = AvgH2CostRatio[
          WMx3[MBRList[[taxq + 1]][[CaseNum]], CostC][[All, All, 2]][[All, 1]]],
       {CaseNum, 1, 3}]]], Flatten[Append[{Which[taxq == 0,
        "Global Clustering as % of Original Network (no tax)", taxq == 1,
        "Global Clustering as % of Original Network (w/ tax)"]},
      Table[PercentForm[SaveList2[[3, taxq + 1, CaseNum]] = ClusteringRatio[
          WMx3[MBRList[[taxq + 1]][[CaseNum]], CostC][[All, All, 2]][[All, 1]]],
       {CaseNum, 1, 3}]]], Flatten[Append[{Which[taxq == 0,
        "Avg Flight Distance as % of Original Network (no tax)", taxq == 1,
        "Avg Flight Distance as % of Original Network (w/ tax)"]},
      Table[PercentForm[SaveList2[[4, taxq + 1, CaseNum]] = AvgDistanceRatio[
          WMx3[MBRList[[taxq + 1]][[CaseNum]], CostC][[All, All, 2]][[All, 1]]],
       {CaseNum, 1, 3}]]]}, Frame → All, Background →
    {{Opacity[0.12, Blue]}, {Opacity[0.12, Blue]}}]]
```


DOI: 10.14324/111.444.2755-0877.1856

In[78]:=
```
AnalysisGrid[[1]]
AnalysisGrid[[2]]
```

Out[78]=

	ρ=2.5%	ρ=3.0%	ρ=5.0%
Avg Passenger Degree as % of Original Network (no tax)	237.9%	239.1%	246.1%
Avg H2 Cost as % of Original Network (no tax)	104.7%	104.4%	104%
Global Clustering as % of Original Network (no tax)	208.94%	208.97%	209.15%
Avg Flight Distance as % of Original Network (no tax)	89.72%	90.05%	88.15%

Out[79]=

	ρ=2.5%	ρ=3.0%	ρ=5.0%
Avg Passenger Degree as % of Original Network (w/ tax)	222.9%	223.8%	232.2%
Avg H2 Cost as % of Original Network (w/ tax)	102.6%	102.6%	103.9%
Global Clustering as % of Original Network (w/ tax)	208.62%	208.64%	208.81%
Avg Flight Distance as % of Original Network (w/ tax)	89.96%	89.53%	90.41%

In[80]:=
```
(*Correlation Between H2 Costs and Passenger Count Degree*)
Correlation[Diagonal[FinalMat[[All, All, 2]]], din[FinalMat[[All, All, 3]]]]
```

Out[80]=
```
0.13976
```

```
(*Barchart of Analysis*)
```

In[81]:=
```
PlotList2 = Table[SaveList2[[All, taxq, i]], {taxq, 2}, {i, 3}];
```

In[82]:=
```
BarChart[Table[Mean[PlotList2[[i]]], {i, 2}],
 ChartLegends → Placed[{"Passenger Degree Ratio", "H2 Cost Ratio",
    "Clustering Ratio", "Flight Distance Ratio"}, Bottom],
 ChartStyle → "Pastel", ChartLabels → {{"No Tax", "€0.55/l Kerosene Tax"}, None},
 Epilog → {Red, Dashed, Line[{{0.6, 1}, {9, 1}}]}, Frame → True]
```

Out[82]=

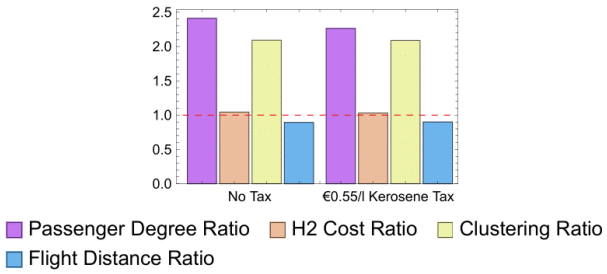


```
(*GeoGraphPlot Set Up*)
```

In[83]:=
```
AC = Table[WMx1[MBRList[[taxq]][[CaseNum]], CostC][[All, All, 3]][[1]],
   {taxq, 1, 2}, {CaseNum, 1, 3}];
```


DOI: 10.14324/111.444.2755-0877.1856

In[84]:=
```
RouteIndex = Flatten[
  Table[Which[FinalMat[[j, k, 3]] == 0, Nothing, FinalMat[[j, k, 4]] == 0, Nothing, True,
    {GeoPosition[{AirportCoordinates[[j, 2]], AirportCoordinates[[j, 3]]}] ↔
      GeoPosition[{AirportCoordinates[[k, 2]], AirportCoordinates[[k, 3]]}],
     j, k}], {j, 1, 345}, {k, 1, 345}]];
RouteIndex2 = Table[{RouteIndex[[j]], RouteIndex[[j + 1]], RouteIndex[[j + 2]]},
  {j, 1, Length[RouteIndex], 3}];
```

In[85]:=
```
BackgroundGraph =
 GeoGraphPlot[Table[RouteIndex2[[j, 1]], {j, 1, Length[RouteIndex2]}],
  VertexSize → 0.2, VertexStyle → Red, GraphLayout → "Geodesic",
  EdgeStyle → Directive[Blue, Thickness[0.0003], Opacity[0.05]],
  GeoRange → {GeoPosition[{77, -27}], GeoPosition[{25, 35}]}]
```

Out[85]=

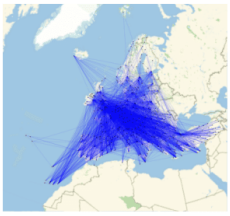

In[86]:=
```
ToPlot2[ListNum_, CaseNum_] :=
 Table[If[MemberQ[AC[[ListNum, CaseNum]], RouteIndex2[[j, 2]]] &&
    MemberQ[AC[[ListNum, CaseNum]], RouteIndex2[[j, 3]]],
   RouteIndex2[[j, 1]], Nothing], {j, 1, 9252}]
```

In[87]:=
```
H2Network[ListNum_, CaseNum_] :=
 Overlay[{BackgroundGraph, GeoGraphPlot[ToPlot2[ListNum, CaseNum],
    EdgeStyle → Directive[Green, Thickness[0.0005], Opacity[0.1]],
    VertexSize → Tiny, VertexStyle → Green, GraphLayout → "Geodesic",
    GeoBackground → GeoStyling[Opacity[0]],
    GeoRange → {GeoPosition[{77, -27}], GeoPosition[{25, 35}]}]}]
```

In[88]:=
```
ArptCoodList = Table[GeoPosition[
    {AirportCoordinates[[j, 2]], AirportCoordinates[[j, 3]]}], {j, 1, 345}];


(*GeoGraphPlot Visualisation*)
```


DOI: 10.14324/111.444.2755-0877.1856

In[89]:=
```
CnvtArpt2 =
  Table[Which[MemberQ[AC[[k, l]], j] && MemberQ[AC[[1, 3]], j], ArptCoodList[[j]] →
     Darker[Green, 0.2], MemberQ[AC[[k, l]], j], ArptCoodList[[j]] → Orange,
    True, ArptCoodList[[j]] → Directive[Red, Opacity[0.05]]],
   {k, 1, 2}, {l, 1, 3}, {j, 1, 345}];
H2ArptMap[ListNum_, CaseNum_] :=
 GeoGraphPlot[Table[RouteIndex2[[j, 1]], {j, 1, Length[RouteIndex2]}],
  VertexShapeFunction → "Point", VertexStyle → CnvtArpt2[[ListNum, CaseNum]],
  GraphLayout → "Geodesic", EdgeStyle → Directive[Opacity[0]],
  GeoRange → {GeoPosition[{77, -27}], GeoPosition[{25, 35}]}]
GraphicsGrid[{{Labeled[H2ArptMap[1, 1], "Progressive Case, No Tax", Top],
   Labeled[H2ArptMap[1, 2], "Central Case, No Tax", Top],
   Labeled[H2ArptMap[1, 3], "Conservative Case, No Tax", Top]},
  {Labeled[H2ArptMap[2, 1], "Progressive Case, Tax", Top],
   Labeled[H2ArptMap[2, 2], "Central Case, Tax", Top],
   Labeled[H2ArptMap[2, 3], "Conservative Case, Tax", Top]}}]
```

Out[91]=

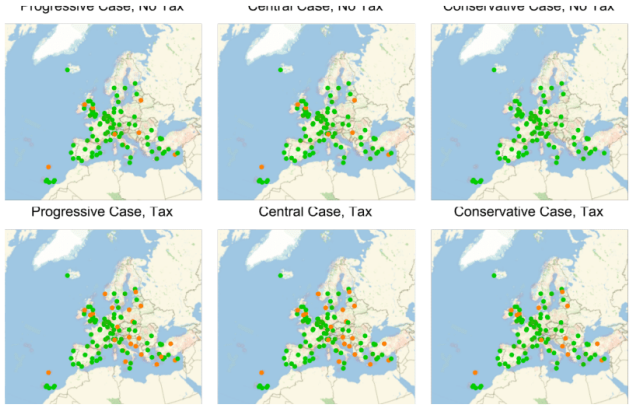

In[92]:=
```
GraphicsGrid[{{Labeled[H2Network[1, 3], "Conservative Case, No Tax", Top],
   Labeled[H2Network[2, 1], "Progressive Case, With Tax", Top]}}]
```

Out[92]=

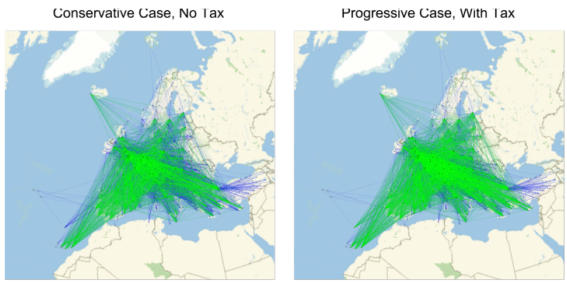

DOI: 10.14324/111.444.2755-0877.1856